

Review

# A Critical Review on the Use of Molecular Imprinting for Trace Heavy Metal and Micropollutant Detection

Patrick Marcel Seumo Tchekwagep <sup>1</sup>, Robert D. Crapnell <sup>2</sup>, Craig E. Banks <sup>2</sup>, Kai Betlem <sup>3</sup>, Uwe Rinner <sup>4</sup>, Francesco Canfarotta <sup>5</sup>, Joseph W. Lowdon <sup>6</sup>, Kasper Eersels <sup>6</sup>, Bart van Grinsven <sup>6</sup>, Marloes Peeters <sup>7,\*</sup> and Jake McClements <sup>7,\*</sup>

- <sup>1</sup> Analytical Chemistry Laboratory, Faculty of Science, University of Yaoundé I, Yaoundé 812, Cameroon; 3omues@gmail.com
  - <sup>2</sup> John Dalton Building, Faculty of Science and Engineering, Manchester Metropolitan University, Chester Street, Manchester M1 5GD, UK; r.crapnell@mmu.ac.uk (R.D.C.); c.banks@mmu.ac.uk (C.E.B.)
  - <sup>3</sup> Department of Microelectronics, Faculty of Electrical Engineering, Mathematics and Computer Science, Delft University of Technology, Mekelweg 4, P.O. Box 616, 2628 CD Delft, The Netherlands; k.betlem@tudelft.nl
  - <sup>4</sup> Institute of Biotechnology, Department of Life Sciences, IMC University of Applied Sciences Krems, Piaristengasse 1, 3500 Krems, Austria; uwe.rinner@fh-krems.ac.at
  - <sup>5</sup> MIP Discovery Ltd., Bedford MK44 1LQ, UK; francesco.canfarotta@mip-dx.com
  - <sup>6</sup> Sensor Engineering Department, Faculty of Science and Engineering, Maastricht University, P.O. Box 616, 6200 MD Maastricht, The Netherlands; joe.lowdon@maastrichtuniversity.nl (J.W.L.); kasper.eersels@maastrichtuniversity.nl (K.E.); bart.vangrinsven@maastrichtuniversity.nl (B.v.G.)
  - <sup>7</sup> Merz Court, School of Engineering, Newcastle University, Claremont Road, Newcastle Upon Tyne NE1 7RU, UK
- \* Correspondence: marloes.peeters@newcastle.ac.uk (M.P.); jake.mcclements@newcastle.ac.uk (J.M.)



**Citation:** Tchekwagep, P.M.S.;

Crapnell, R.D.; Banks, C.E.; Betlem, K.; Rinner, U.; Canfarotta, F.; Lowdon, J.W.; Eersels, K.; van Grinsven, B.; Peeters, M.; et al. A Critical Review on the Use of Molecular Imprinting for Trace Heavy Metal and Micropollutant Detection. *Chemosensors* **2022**, *10*, 296. <https://doi.org/10.3390/chemosensors10080296>

Academic Editor: Pi-Guey Su

Received: 8 June 2022

Accepted: 12 July 2022

Published: 27 July 2022

**Publisher's Note:** MDPI stays neutral with regard to jurisdictional claims in published maps and institutional affiliations.



**Copyright:** © 2022 by the authors. Licensee MDPI, Basel, Switzerland. This article is an open access article distributed under the terms and conditions of the Creative Commons Attribution (CC BY) license (<https://creativecommons.org/licenses/by/4.0/>).

**Abstract:** Molecular recognition has been described as the “ultimate” form of sensing and plays a fundamental role in biological processes. There is a move towards biomimetic recognition elements to overcome inherent problems of natural receptors such as limited stability, high-cost, and variation in response. In recent years, several alternatives have emerged which have found their first commercial applications. In this review, we focus on molecularly imprinted polymers (MIPs) since they present an attractive alternative due to recent breakthroughs in polymer science and nanotechnology. For example, innovative solid-phase synthesis methods can produce MIPs with sometimes greater affinities than natural receptors. Although industry and environmental agencies require sensors for continuous monitoring, the regulatory barrier for employing MIP-based sensors is still low for environmental applications. Despite this, there are currently no sensors in this area, which is likely due to low profitability and the need for new legislation to promote the development of MIP-based sensors for pollutant and heavy metal monitoring. The increased demand for point-of-use devices and home testing kits is driving an exponential growth in biosensor production, leading to an expected market value of over GBP 25 billion by 2023. A key requirement of point-of-use devices is portability, since the test must be conducted at “the time and place” to pinpoint sources of contamination in food and/or water samples. Therefore, this review will focus on MIP-based sensors for monitoring pollutants and heavy metals by critically evaluating relevant literature sources from 1993 to 2022.

**Keywords:** biomimetics; sensors; molecularly imprinted polymers; environmental monitoring; heavy metals

## 1. Need for Biomimetics

Biosensors rely on biological elements for detection such as antibodies, enzymes, or cells. However, these natural recognition elements possess inherent drawbacks. For antibodies, these include limited stability, high cost, and considerable batch-to-batch variation. Consequently, this can lead to waste of resources and unreliable data. Of all antibodies on

the market, it has been reported that up to 75% have not been validated, show a low level of validation, or do not perform adequately for the intended application [1]. There are also ethical concerns regarding the use (and subsequent sacrifice) of animals for traditional antibody production. Despite improvements in validation strategy and significant investment from industry, there is still a large dependence on animal-derived antibodies. In fact, the number of animals used for antibody generation in Europe alone is estimated at around one million per year, meaning that there is a strong drive towards finding antibody replacements [2]. A new recommendation was released in 2020 on non-animal-derived antibodies from the European Union (EU) Reference Laboratory, which calls for the replacement of animal-derived antibodies where possible and is expected to have an important impact on the future of antibody production in the EU.

One method to replace natural receptors is by using smaller counterparts that are more stable. These are referred to as “antibody mimics” since they have similar functions to antibodies despite being structurally different. An example of these are affibodies which consist of three  $\alpha$ -helices with a molar mass of ~6 kDa, whereas the molar mass of a typical monoclonal antibody is ~150 kDa. This reduction in size leads to affibodies being able to withstand extreme conditions such as high temperatures and wide ranges of pH [3]. Affibodies have received Food and Drug Administration approval for therapeutic applications. However, they are expensive and their market availability is limited, which is likely due to the lack of a platform technology for purification [4].

Another “antibody mimic” example is single-chain variable fragments (scFvs), which are fusion proteins from the variable regions of the heavy and light chains of immunoglobulins connected via a short linker peptide. Therefore, this is the smallest fragment of an antibody that can retain the same antigen-binding specificity [5]. One of the main advantages of scFvs is that they can be produced in large quantities using straightforward and low-cost expression systems such as *Escherichia coli*. In contrast, monoclonal antibodies require complicated mammalian expression systems and extensive post-translational modification. Antigen-binding fragments (Fabs) are larger than scFvs (molar masses of ~50 and 28 kDa, respectively), and are composed of the whole light chain and the variable region of the heavy chain of an antibody. The discovery of suitable scFvs and Fabs has been augmented due to advances in phage display techniques, which are versatile in vitro technologies for the rapid selection of high affinity antibodies or antibody fragments. The ability for multifaceted selection to build large libraries, in addition to the stimulus of the 2018 Nobel Prize in Chemistry being awarded to phage display is expected to increase the range of commercial products. While the primary focus for these antibody mimics has been for therapeutic applications, there is interest within the biosensing community towards using these materials as recognition elements. The advantage of Fab fragments for this application is their low-cost and easy development (several days), while scFvs offer the advantage of high customizability that will improve sensitivity [6]. However, these fragments can denature upon immobilization to sensor surfaces and in general, synthetic recognition elements demonstrate higher specificity.

Aptamers are single-stranded oligonucleotides or peptide molecules that fold into defined architectures, and therefore can specifically and selectively bind target molecules. The binding affinity of aptamers is comparable, if not better than monoclonal antibodies if sufficient time can be set aside to optimize development [7]. This is also the downfall of the method as there are significant costs associated with the optimization process. However, the method generally utilized to generate aptamers known as systematic evolution of ligands by exponential enrichment (SELEX) has led to advances in efficiency and reliability. There are up to six different SELEX methods available that can be tailored towards different targets. A review by Zhang et al. [8] compares these different methods against each other, highlighting key aspects and (dis)advantages. Considering aptamer synthesis is low-cost and selection strategies have been improved, the technology has experienced a surge in popularity. Aptamers can be chemically modified at the 3' or 5' end (commonly with an amine or thiol group) to enable facile surface immobilization. However, care must be

taken that this does not interfere with their analyte-binding ability since binding is based on conformational changes. While DNA aptamers offer enhanced stability compared to antibodies, they are still subject to nuclease degradation [9]. This has led to novel hybrid-systems with enhanced stability, which is achieved by incorporating polymeric elements via either chemical modification of the structure or formation of electropolymerized polymers around the aptamers to lock them in place [10,11].

Since 2010, there has been an exponential increase in the number of publications on aptamers, particularly in the detection of proteins [12]. A similar trend is followed by MIPs, which are polymeric recognition elements. While the structure of MIPs is vastly different to antibodies, the functional groups of some monomers that are used as building blocks do bear similarities to natural amino acids. Therefore, one can think of the binding site of a MIP as having similarities to the active site of an enzyme, where the polymer network serves as the 3D structure to stabilize the active site [13]. It is clear that MIPs can surpass some other synthetic recognition elements in terms of cost and stability; for instance, they are not degraded by nucleases in the body. Due to the generic nature of the technology which allows for detection of virtually any target, MIPs are commercially viable and possess the potential to make a significant contribution to the market [14]. MIP Technologies (AFFINIMIPSPE products), Supelco (Merck), and Acros (SupelMIP) have pioneered MIPs for purification and separation. Aspira Biosystems sell MIPs to selectively capture microorganisms. Companies selling MIPs for the diagnostics market include MIP Discovery and Sixth Wave.

However, MIPs need to find niche applications compared to natural receptors to stimulate uptake which, in addition to lack of mass-production facilities, is currently limiting their commercial potential. We expect that in the coming years, there will be a surge of biomimetic receptors on the market with aptamers initially beginning to compete with antibodies and enzymes.

## 2. Introduction to MIPs

MIPs are synthetic materials with a high affinity towards specific molecules. This affinity originates from distinct cavities in their polymeric matrix, which are generated by the inclusion of guest molecules (templates) during the polymerization process. After polymerization, the template molecules are removed and leave behind molecular imprints, which meet the spatial requirements (both in terms of size and arrangement of functional groups) of the template molecules and allow for an effective binding of these molecules with the modified polymer. Removal is commonly performed by solvent extraction, but other options include physically assisted extraction methods or use of subcritical/supercritical solvents [15]. Different binding modes are responsible for an efficient interaction of the cavity and requisite template. The most common method in recent years, the non-covalent approach, uses interactions such as ionic interactions, hydrogen bonds,  $\pi$ - $\pi$  interactions, van der Waals forces, metal coordination interactions, and hydrophobic interactions. The greater the variety and number of interactions between the imprint species and functional monomer, the better the artificial binding site becomes. This process is described in detail in ref [16]. Generally, the interaction between the polymer and template follows the principle of a “molecular lock and key” as initially postulated by Emil Fischer as early as 1894, and thus strongly correlates with antibody–antigen interactions [17]. In this respect, MIPs represent artificial receptors, mimicking their natural counterparts using semi-covalent interactions to bind targets. However, the binding of MIPs can follow different approaches, including covalent interactions and chelation with metals [18]. The success story of MIPs dates back to the early 1930s when Polyakov first observed distinct differences in silica due to different solvents being present during the drying process [19]. Some years later, another interesting observation was made by Dickey who prepared silica gel in the presence of azo dyes [20]. This report and similar findings initiated some research in the field of MIPs, but the overall number of publications remained quite limited. However, this changed

dramatically in the late 1980s when the research area was revived by the pioneering work of Mosbach and Wulff, among others [21–24].

The preparation of MIPs is schematically outlined in Figure 1. Monomeric building blocks are mixed with template molecules before the polymerization process takes place, giving the molecules chance to assemble around the template [21,22,25]. The orientation of the individual building blocks is then locked in place during the cross-linking of the monomers, generating an imprint with the size, shape, and electrostatic surface profile of the template molecule. To evaluate the specificity of MIPs, the synthesis process is duplicated in the absence of the template, producing a reference non-imprinted polymer (NIP) or alternatively by performing the imprinting process in the presence of a similar template.

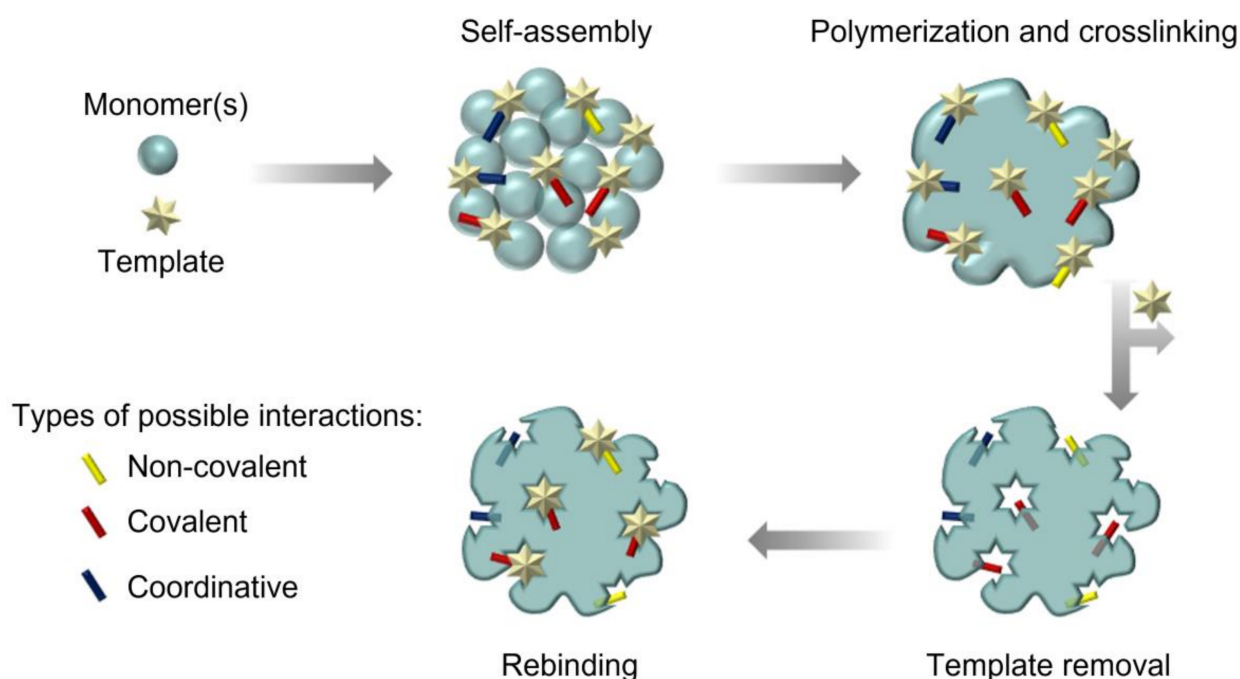


**Figure 1.** Schematic representation of MIP synthesis.

The polymerization step is crucial for the molecular recognition of the template molecules. Firstly, the choice of the monomer and cross-linker employed in the polymerization has significant impact on the level of molecular recognition between the polymeric matrix and template molecule. The overall polarity must be considered carefully as effective binding between a completely non-polar polymer and a highly oxygenated natural product is unlikely. Furthermore, the reaction of the template molecule with the monomeric building blocks during the polymerization needs to be avoided. Many different monomers are currently commercially available, facilitating a tailor-made solution to individual requirements and templates with various complexities and surface properties. The selection process of the optimal polymer formulation is now often assisted by computational methods, which have gained considerable importance in the design of MIPs [26]. First employed in the late 1990s and early 2000s, *in silico* aided design of MIPs has significantly advanced over the last few years [27]. Today, quantum mechanical modeling and semi-empirical methods are routinely used to guide the synthesis and application of MIPs [28].

Different polymerization protocols have been employed in the production of MIPs. For example, bulk polymerization is a simple and well-established process that is commonly utilized for MIP preparation. After the polymerization, the obtained polymer material is ground to obtain small particles with well-defined size and large surface area, which is required to enhance binding site accessibility and allow the target to bind to the imprinted cavities. Properties of the MIP significantly depend on the pore size and cross-linking of the polymer. If the functional groups in the matrix are too flexible, the required level of



selectivity towards the template molecule is not reached in the final product. Nanoparticles present an interesting alternative to bulk polymerization as they often exhibit superior performance due to their higher surface-area-to-volume ratios [29]. However, they are more difficult to produce in large quantities, which presents a significant disadvantage. Precipitation polymerization has commonly been employed in the preparation of MIP nanoparticles [30]. Alternatively, emulsion polymerization takes advantage of high-shear homogenization of the monomers in the presence of co-surfactants and often produces nanoparticles in higher yield [31]. Core-shell emulsion polymerization and grafting are well-suited for the preparation of complex nanoparticles with polymer layers deposited on various materials [32,33]. Micro- and nano-gels are cross-linked unimolecular particles, which are mostly soluble and produced via extensive grinding or high-dilution polymerization. They are designed for special applications, such as catalytic processes and biological systems [34,35]. Imprinting of larger biomolecules is more complex and thus more sophisticated protocols, such as the polymerization packed bed method, are often used to obtain hierarchically structured polymers [36]. In recent years, solid-phase methods were also developed for the preparation of molecularly imprinted polymer nanoparticles (nanoMIPs). Covalently immobilized template molecules on the surface of a solid support, such as glass beads, allow the synthesis of template-free nanoMIPs with high affinity for even large biomolecules [13]. However, the process becomes progressively more challenging with the increasing molecular weight of the template molecule, and therefore surface imprinting technologies are preferred for larger biomolecules, viruses, cells, or cell fragments/epitopes (substructure imprinting) [37,38].

Before MIPs can be employed in sensor technology, the template and any unreacted monomer must be removed. The efficiency of standard extraction protocols, such as Soxhlet extraction or incubation of the MIP in a solvent that induces swelling, can further be improved upon by physically assisted extraction protocols [25,39]. Ultrasound, microwave irradiation, or mechanical stirring are suited to increase efficiency while decreasing the extraction time [40–42]. Alternatively, extraction with subcritical water or supercritical carbon dioxide has been described [15,43]. Further details on MIP preparation can be found in refs [16,44,45]. MIPs have been developed with high selectivity towards ions and molecules, in addition to larger units such as viruses, cell fragments, or cells. The selectivity of MIPs is comparable, sometimes even superior, to traditional analytical protocols and these compounds constitute a cost-effective alternative, which often allows for the quantitative on-site determination of analytes. The following sections summarize applications of MIP-based sensors in the determination of heavy metals and other problematic pollutants using electrochemical and optical detection methods.

### 3. MIP-Based Sensing of Heavy Metals

Electrochemical detection is focused on measuring changes in the electrical signal, which occur when chemicals interact with a sensing surface. There are three main electrochemical approaches used in MIP-based sensors (Figure 2). First, there is a direct determination of the redox-active analyte where the recorded faradaic current comes from direct electron transfer between the target and electrode surface. Secondly, an indirect quantification can be used via the generation of a redox-active product, which subsequently reacts at the electrode surface. Thirdly, another indirect quantification method is using a redox marker such as ferri/ferrocyanide. In this case, the diffusional permeability of the redox marker through the electrode surface is monitored. Electrochemical detection is an especially attractive technique because of its high specificity, experimental simplicity, low cost, and easy integration into portable devices. Consequently, it is unsurprising that the technique is commonly utilized within commercial sensors. In the next section, we discuss the detection of heavy metals and touch on relevant screen-printing technology, which has attracted considerable commercial interest due its low-cost and compatibility with mass-manufacturing.

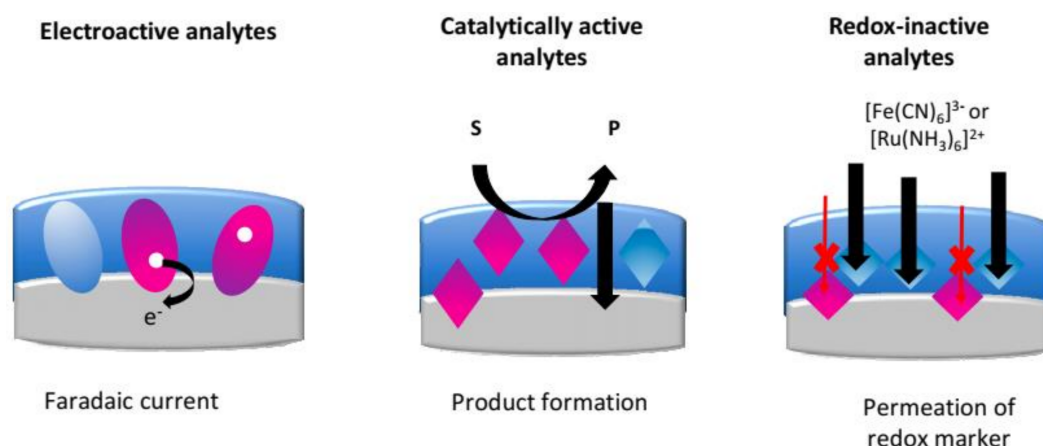


**Figure 2.** Schematic outlining the main detection methods used in electrochemical MIP-based sensors. Figure reproduced from [46].

### 3.1. Determination of Heavy Metals

The term heavy metal describes a group of metals and metalloids with high atomic weight and density. Heavy metals are an extremely problematic class of contaminants, which can cause considerable damage to human health and the environment [47]. Mercury, cadmium, copper, and lead are heavy metals commonly found in domestic and wastewater [48]. In the literature, it is well demonstrated that once inside an organism, these metals can bind to proteins, displace inherent metal proteins, and bioaccumulate, which can cause various diseases and disorders [48]. To address the negative environmental and health impacts of heavy metal contamination, safe limits must be outlined by governmental organizations such as the EU and World Health Organization (WHO) [49]. For instance, the EU reviewed the heavy metal limits in drinking water (Table 1) through the “Right2Water” campaign in 2020 [50]. To meet these thresholds, scientists must develop methods to remove and control the level of contaminants in the environment.

**Table 1.** EU drinking water guidelines as of 2020 [50].

Metal	Previous EU Limit ( $\mu\text{g}\cdot\text{L}^{-1}$ )	New EU Limit ( $\mu\text{g}\cdot\text{L}^{-1}$ )
Antimony	5	5
Arsenic	10	10
Cadmium	5	5
Chromium	50	25
Copper	2000	2000
Lead	10	5
Mercury	1	1
Nickel	20	20
Selenium	40	10
Uranium	30	30

Atomic absorption spectrometry [51], mass spectrometry [52], induced coupled plasma mass spectrometry [53], X-ray fluorescence [54], and various optical methods [55,56] are well established techniques for accurate determination of heavy metals in the environment and food. However, whilst these techniques can detect heavy metals at the concentration range set by policies, they have several distinct disadvantages such as laborious sample preparation, high equipment costs, steep learning curves of users, and lack of portability. Therefore, the determination of heavy metals using electrochemical techniques

can be considered as more advantageous since the core equipment used (a potentiostat) is cheap and analysis can be performed on-site and in real time [49]. Ion imprinted polymers (IIPs) are MIPs that specifically use ions as the template. They were first introduced by Nishide et al. [57] in 1976 where poly(4-vinylpyridine) was cross-linked with 1,4-dibromobutane in the presence of metal ions ( $\text{Cu}^{2+}$ ,  $\text{Fe}^{3+}$ ,  $\text{Co}^{2+}$ ,  $\text{Zn}^{2+}$ ,  $\text{Ni}^{2+}$ , and  $\text{Hg}^{2+}$ ), which acted as a template. The general procedure for IIP synthesis involves the preparation of a ligand–metal complex and its subsequent copolymerization with a cross-linker in order to create three-dimensional recognition cavities inside the polymer network (Figure 3) [58].

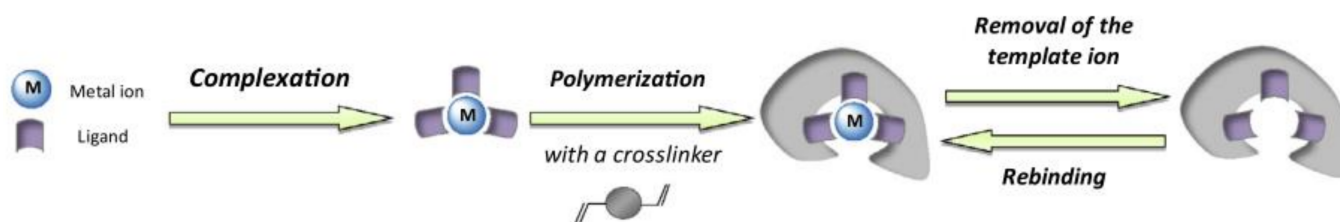


**Figure 3.** Schematic representation of IIP synthesis. Figure reproduced from [58] with permission from copyright Elsevier 2013.

To improve the sensitivity and selectivity of electrodes for electroanalysis, IIPs are frequently fabricated to target specific heavy metals. The role of IIPs is similar to solid-phase extraction in that they are utilized to preconcentrate the given heavy metal ion onto the electrode, thus enhancing the stripping signals. A brief scheme of the mechanism of detection in an IIP-based electrochemical sensor is shown in Figure 4. In the following sections, we will review recent developments in IIP-based electrochemical sensors for the detection of three of the most hazardous heavy metals: mercury(II), cadmium(II), and lead(II).

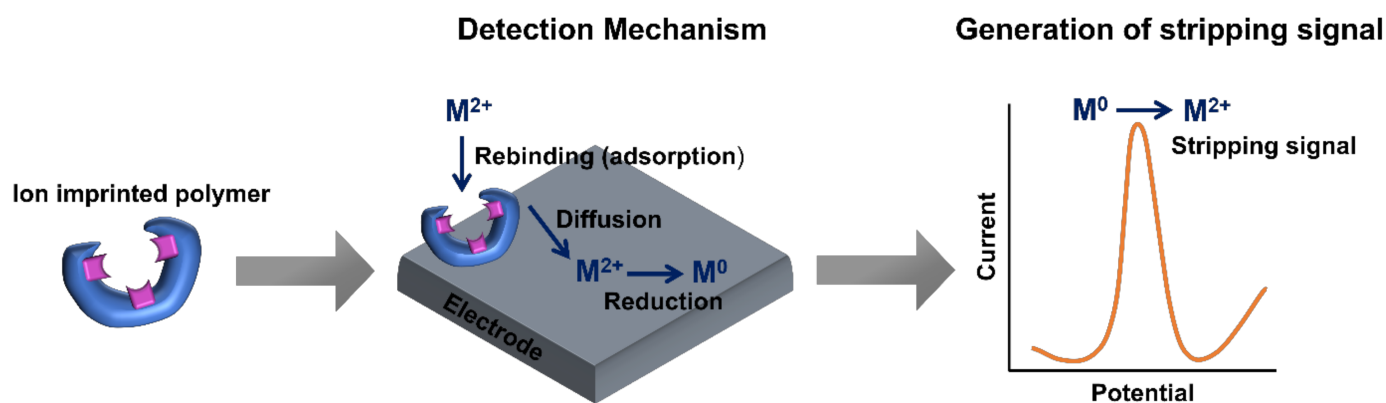


**Figure 4.** Schematic representation of the detection mechanism of electrochemical IIP-based sensors.

### 3.1.1. Detection of Lead(II)

Plumbing systems are the primary source of lead contamination in drinking water. As a highly hazardous heavy metal, lead can accumulate in living organisms and cause severe poisoning [59]. Intensive exposure to lead is particularly harmful for the cognitive development of young children [60]. In order to lower the incidence of lead poisoning, the WHO has systematically reduced the legal threshold of lead in drinking water (100 to 50 to  $10 \mu\text{g}\cdot\text{L}^{-1}$ ) over the last two decades [61]. Within the literature, there are relatively few investigations from only a small number of research groups that focus on developing electrochemical sensors using IIPs for heavy metal detection in the environment (Table 2 summarizes those focused on lead(II) detection).

**Table 2.** Summary of studies which have utilized IIPs for the electrochemical detection of lead(II).

Target/Synthesis	Electrode <sup>a</sup>	Detection Method <sup>b</sup>	Dynamic Concentration Range (nM)	LoD <sup>c</sup> (nM)	Samples	Ref.
-Pb(CO <sub>3</sub> ) <sub>2</sub> -Copolymerization	CPE	DPSV	1–810	0.6	-Tap/river/waste H <sub>2</sub> O -Edible Salt	[62]
-Pb(NO <sub>3</sub> ) <sub>2</sub> -Precipitation polymerization	CPE	DPSV	1–10 10–10,000	0.03	-Distilled/tap/sea/ waste H <sub>2</sub> O	[63]
-Pb(CH <sub>3</sub> COO) <sub>2</sub> -Thermal precipitation polymerization	CPE	DPV	0.3–1 10–1000	0.1	-Tap H <sub>2</sub> O -Lipstick	[64]
-Pb(NO <sub>3</sub> ) <sub>2</sub> -Free radical polymerization	GCE	DPV	50–60,000 0–1000	10	-Waste/pool H <sub>2</sub> O -Rice	[65]
-Pb(ClO <sub>4</sub> ) <sub>2</sub> -Copolymerization	GCE/MWCNTs	SWV	0.01–0.5 1–80	0.0038	-Sea/river H <sub>2</sub> O	[66]
-Pb(CO) <sub>3</sub> -Precipitation polymerization	CPE	DPV	1–750	0.013	-Tap/river H <sub>2</sub> O -Flour -Rice	[67]
-Pb(NO <sub>3</sub> ) <sub>2</sub> -Precipitation polymerization	GCE	DPASV	2.4–60 70–100	0.77	-Tap/mineral H <sub>2</sub> O -Physiological serum -Synthetic urine	[68]
-Pb(NO <sub>3</sub> ) <sub>2</sub> -Free radical polymerization	Platinum	DPV	4800–24,100	20	-Lake H <sub>2</sub> O -Mining effluent -Food -Cosmetics	[69]
-Pb(CH <sub>3</sub> COO) <sub>2</sub> -Thermal precipitation polymerization	CPE	DPASV	0.4–10 10–1000	0.11	-Tap/well H <sub>2</sub> O -Seronorm™ urine	[70]
-Pb(NO <sub>3</sub> ) <sub>2</sub> -Precipitation polymerization	GCE	DPV	0.48–24.1 24.1–390	0.24	-Tap/rain/river H <sub>2</sub> O -Fruit juice	[71]
-Pb(CH <sub>3</sub> COO) <sub>2</sub> -Thermal precipitation copolymerization	Graphite electrode	Potentiometry	0.53–1 × 10 <sup>8</sup>	0.34	-Tap/well/river/ mineral H <sub>2</sub> O	[72]

<sup>a</sup> Carbon paste electrode (CPE); glassy carbon electrode (GCE); multiwalled carbon nanotubes (MWCNTs).

<sup>b</sup> Differential pulse stripping voltammetry (DPSV); differential pulse voltammetry (DPV); square wave voltammetry (SWV); differential pulse anodic stripping voltammetry (DPASV). <sup>c</sup> Limit of detection (LoD).

Alizadeh et al. [62] synthesized a novel nano-structured IIP of methacrylic acid–Pb<sup>2+</sup> complex and ethylene glycol dimethacrylate (EGDMA) using precipitation polymerization. The obtained IIPs were used to modify CPEs for the detection of lead(II), with a LoD of 0.6 nM (signal to noise (S/N) = 3). The sensor was successfully applied for the detection of trace lead(II) in various water samples and edible salts. Bojdi et al. [63] reported on the synthesis of lead(II) IIPs by precipitation polymerization of 4-vinylpyridine (functional monomer), EGDMA (cross-linker), 2,2'-azobisisobutyronitrile (AIBN, initiator), 4-(2-pyridylazo)resorcinol (lead-binding ligand), and lead(II) (template) in acetonitrile solution. The sensor showed high selectivity for lead(II) in the presence of common metal ion interferents. The LoD of the sensor was 30 pM (S/N = 3) and the sensor was effectively utilized for trace detection of lead(II) in spiked environmental water samples. Hu et al. [65] synthesized an IIP for lead(II) using methyl methacrylate as the functional monomer. Distinct interference on lead(II) detection was observed when the ratio of various contaminants to lead(II) was greater than 60. The sensor also exhibited consistently favorable performance (relative standard deviation of 3.8%) with two dynamic concentration ranges from 0.05 to 60 μM and 0.0 to 1 μM, and a LoD of 0.01 μM. The sensor was successfully used for lead(II) determination in waste pool water and rice.

To improve sensor performance in the detection of lead(II), some researchers have introduced materials to increase the surface area of the reaction and/or transfer of electrons. For instance, an itaconic acid-Pb<sup>2+</sup> complex and EGDMA were copolymerized to obtain an IIP material. The IIP was then impregnated with a small amount of MWCNTs (6% *w/w*) to modify a CPE for the detection of lead(II) in aqueous solutions [71]. The sensor exhibited a LoD of 3.8 pM (S/N = 3) and two linear concentration ranges from 10 pM to 0.5 nM and 1 to 80 nM. However, a 50-fold excess of Fe<sup>2+</sup> and Zn<sup>2+</sup>, as well as a 40-fold excess of Cu<sup>2+</sup> had a detrimental effect on the sensor response [66]. Similarly, Dahaghin et al. [71] grafted IIP onto Fe<sub>3</sub>O<sub>4</sub>@SiO<sub>2</sub> nanomaterials. This synthesis used 2-(2-aminophenyl)-1H-benzimidazole and 4-vinylpyridine as a ligand and functional monomer, respectively. The obtained polymer was utilized in the modification of GCEs for the detection of lead(II), with the sensor exhibiting a LoD of 0.24 nM (S/N = 3). This modified GCE was subsequently used for determining lead(II) in water and fruit juice.

### 3.1.2. Detection of Mercury(II)

Mercury exposure constitutes a significant health and environmental hazard. It tends to bioaccumulate in the environment and can cause serious damage to the central nervous and reproductive systems [73,74]. In 2007, the WHO set the mercury threshold concentration at 6 µg·L<sup>-1</sup> (30 nM) in drinking water [61]. A comprehensive screening of the literature reveals that only a small number of papers have reported on the detection of mercury(II) using IIP-based electrochemical sensors (Table 3).

**Table 3.** Summary of studies which have utilized IIPs for the electrochemical detection of mercury(II).

Target/Synthesis	Electrode <sup>a</sup>	Detection Method <sup>b</sup>	Dynamic Concentration Range (nM)	LoD (nM)	Samples	Ref.
-Hg(NO <sub>3</sub> ) <sub>2</sub> -Free radical polymerization	CPE	DPV	2.5–5000	0.52	-Tap/river/waste H <sub>2</sub> O	[75]
-HgCl <sub>2</sub> -Thermal precipitation polymerization	GCE	DPASV	10–70,000	5	-Waste/ground H <sub>2</sub> O	[76]
-HgCl <sub>2</sub> -Free radical polymerization	CPE	Potentiometry	4–130,000	1.95	-Tuna fish -Shrimp -Human hair	[77]
-Hg(CH <sub>3</sub> COO) <sub>2</sub> -Thermal precipitation polymerization	CILE	DPASV	0.5–10 80–2000	0.1	-Municipal/ industrial/petrochemical waste H <sub>2</sub> O	[78]
-Hg(NO <sub>3</sub> ) <sub>2</sub> -Free radical polymerization	GCE	SWASV	0.35–400	0.1	-Tap/aqueduct/ waste/river H <sub>2</sub> O	[79]
-Hg <sup>2+</sup> -Free radical polymerization	CPE	SWV	1–17.5 3–8000	0.2	-River/water H <sub>2</sub> O -Potato/carrot/lettuce	[80]
-HgCl <sub>2</sub> -Thermal precipitation polymerization	CPE/MWCNT	SWV	0.1–20	0.029	-River/sea H <sub>2</sub> O	[81]
-HgCl <sub>2</sub> -Thermal precipitation polymerization	GCE	SWASV	0.1–4000	0.5	-Tap/ground/ waste H <sub>2</sub> O	[82]
-HgCl <sub>2</sub> -Precipitation polymerization	CPE	SWASV	0.06–25	0.018	-Tap/sea H <sub>2</sub> O	[83]



Table 3. Cont.

Target/Synthesis	Electrode <sup>a</sup>	Detection Method <sup>b</sup>	Dynamic Concentration Range (nM)	LoD (nM)	Samples	Ref.
-HgCl <sub>2</sub> -Precipitation polymerization	CPE	Potentiometry	1–1000	0.43	-Tap/sea H <sub>2</sub> O	[84]
-HgCl <sub>2</sub> -Electropolymerization	Gold	SWV	0.001–1000	0.001	-Tap/ground/ waste H <sub>2</sub> O	[85]

<sup>a</sup> Carbon ionic liquid paste electrode (CILE). <sup>b</sup> Square wave anodic stripping voltammetry (SWASV).

Alizadeh et al. [75] described a simple and selective IIP-based electrode for the detection of mercury(II) in real samples. Vinyl pyridine, acting as both the functional monomer and complexing agent, interacted with mercury(II) in the presence of the initiator. The CPE modified with the prepared polymer was utilized to detect mercury(II) in tap, river, and lake water. The group enhanced selectivity of the mercury(II) sensor by including another functional monomer (itaconic acid) and a different synthesis method involving precipitation polymerization [81]. Bahrami et al. [78] prepared a voltametric sensor for sensitive and selective mercury(II) detection using a CILE impregnated with Hg<sup>2+</sup>-IIP nanobeads. Additionally, the non-conductive organic binder usually added to form the carbon paste was replaced by a carbon ionic liquid, which assisted in increasing electrode conductivity. This sensor could detect low mercury(II) levels in complex mixtures and exhibited a wide concentration range (1–2000 nM). Ait-Touchente et al. [85] developed an IIP electrochemical sensor based on surface modification of gold electrodes with diazonium salt and the growth of ZnO nanorods. This was followed by electropolymerization of the pyrrole in the presence of mercury(II) (template) and L-cysteine (cross-linker). A LoD of 1 pM was obtained, making it the most sensitive mercury(II) detection method to date.

### 3.1.3. Detection of Cadmium(II)

Cadmium is toxic and has a propensity to bioaccumulate; prolonged cadmium exposure is linked to severe health implications, particularly damage to the bones, lungs, and kidneys [86]. The WHO has set the threshold cadmium(II) concentration in drinking water at 3 µg·L<sup>-1</sup> (26.7 nM) [61]. Similarly to lead(II) and mercury(II), there is relatively sparse literature on electrochemical detection of cadmium(II) using IIP-based sensors and it is generally produced by a small number of research groups (Table 4). For example, the group of Alizadeh et al. [87] has also been active in cadmium(II) detection, modifying CPEs with IIPs to obtain sensors with a LoD of 0.52 nM (S/N = 3). The sensor had high selectivity as a 500-fold molar excess of different alkaline and earth alkaline cations did not significantly influence the detection of 50 nM of cadmium(II), and detection in real water samples was possible. Dahaghin et al. [88] prepared a cadmium(II) IIP by co-precipitation polymerization using a range of monomers in acetonitrile, which were subsequently applied to GCEs. Cations such as Zn<sup>2+</sup>, Cr<sup>3+</sup>, Pb<sup>2+</sup>, Ni<sup>2+</sup>, Ag<sup>+</sup>, Hg<sup>2+</sup>, and K<sup>+</sup> at 100-fold molar excess of 0.03 µM cadmium(II) did not meaningfully influence cadmium(II) detection. The LoD was 0.1 nM and the electrode was successfully utilized for cadmium(II) detection in waste, river, and tap water. Recently, the natural polymer chitosan was used by Wu et al. [89] as a base substrate for the synthesis of cadmium(II) IIPs. The results demonstrate that the voltammetry response of cadmium(II) at 0.09 µM was slightly perturbed in the presence of 20-fold other cations. The electrode exhibited a good linear response towards cadmium(II) in the range of 0.1 to 0.9 µM with a LoD of 0.17 nM.

**Table 4.** Summary of studies which have utilized IIPs for the electrochemical detection of cadmium(II).

Target/Synthesis	Electrode	Detection Method	Dynamic Concentration Range (nM)	LoD (nM)	Samples	Ref
-Cd(NO <sub>3</sub> ) -Free radical polymerization	CPE	Potentiometry	0.1–67,000	100	-Industrial waste H <sub>2</sub> O	[90]
-Cd(NO <sub>3</sub> ) -Free radical polymerization	CPE	DPV	1–500	0.52	-Tap/lake H <sub>2</sub> O	[87]
-Cd(NO <sub>3</sub> ) <sub>2</sub> -Bulk polymerization	CPE	DPSV	17.8–1800	2.76	-Tap/well/sea H <sub>2</sub> O -Rice -Tomato sauce	[91]
-CdCl <sub>2</sub> -Thermal copolymerization	Graphite	Potentiometry	200–1 × 10 <sup>7</sup>	100	-Tap H <sub>2</sub> O	[92]
-Cd(NO <sub>3</sub> ) <sub>2</sub> -Free radical polymerization	CPE	DPV	89.8–24,000 24,500–59,500 59,500–174,500	44	-Tap/mineral/ lake H <sub>2</sub> O	[93]
-CdCl <sub>2</sub> -Sol-gel method	CPE	DPASV	4.4–400	1.33	-Tap/river/dam/ waste/aqueduct H <sub>2</sub> O	[94]
-Cd(NO <sub>3</sub> ) <sub>2</sub> -Coprecipitation polymerization	GCE	DPV	8–50 50–800	0.1	-Tap/river/waste H <sub>2</sub> O	[88]
-CdCl <sub>2</sub> -Free radical polymerization	Platinum	DPV	8900–44,500	30	-Lake H <sub>2</sub> O -Pigments -Cosmetics -Fertilizer	[95]
-Cd <sup>2+</sup> -Bulk copolymerization	CPE	DPASV	4–500	1.94	-Tap/river/ mineral H <sub>2</sub> O -Rice -Blood/urine	[96]
-CdSO <sub>4</sub> -Electropolymerization	GCE	SWASV	8.9–900	2.3	-Lake/river H <sub>2</sub> O	[97]
-CdCl <sub>2</sub> - Electropolymerization	GCE	DPV	100–900	0.17	-Tap/river H <sub>2</sub> O -Milk	[89]
-CdSO <sub>4</sub> -Electropolymerization	GCE	SWASV	8.9–400	1.2	-Lake/river H <sub>2</sub> O	[98]

This literature review reveals that there are relatively few papers from only a small number of research groups that discuss the performance of IIP-based electrochemical sensors for heavy metal detection. One reason for the lack of research in this area may be the limited possibilities to innovate the synthesis protocol of IIPs. However, from these papers, it is clear that IIP-based sensor performance is consistently improved by increasing surface area and/or electron transfer by embedding conductive materials, (e.g., SiO<sub>2</sub> and Fe<sub>2</sub>O<sub>3</sub> nanoparticles, graphene, MWCNTs) into the electrode surface [99]. Precipitation polymerization is most commonly used for IIP synthesis, which is likely because nanosized particles are produced with a high number of adsorption sites per particle. Stripping voltammetry is typically utilized as an electrochemical detection method with DPV generally being favored over SWV. It is clear that potentiometric methods of detection offer a very large domain of linearity compared to amperometric methods. Furthermore, this review highlights that casting the prepared IIP material on a solid electrode and blending the IIP with graphite are the two main approaches used for the integration of IIPs with transducers. In the former case, GCEs are most commonly used, whereas in the latter, CPEs are generally favored. The reason for this may be that the imprinted material has poor adherence to the GCE, which would make sample preparation more difficult. An interesting avenue for future

research is developing IIP sensor arrays, which can simultaneously detect multiple heavy metals. This is particularly relevant as numerous heavy metals are generally present in real samples. Roy et al. [100] performed a unique study that assessed the simultaneous detection of cadmium(II), lead(II), and copper(II) using a multi-template imprinting technique (Figure 5). For this, an imprinted nanowire was synthesized using MWCNTs as a core on which a layer of conducting polyarginine was cast using an electropolymerization technique. The reduction peak potentials of the cadmium(II), lead(II), and copper(II) on the pencil graphite electrode modified with the imprinted nanowire were separated completely into three well-defined peaks at 0.00,  $-0.20$ , and  $-0.56$  V vs. Ag/AgCl, respectively.

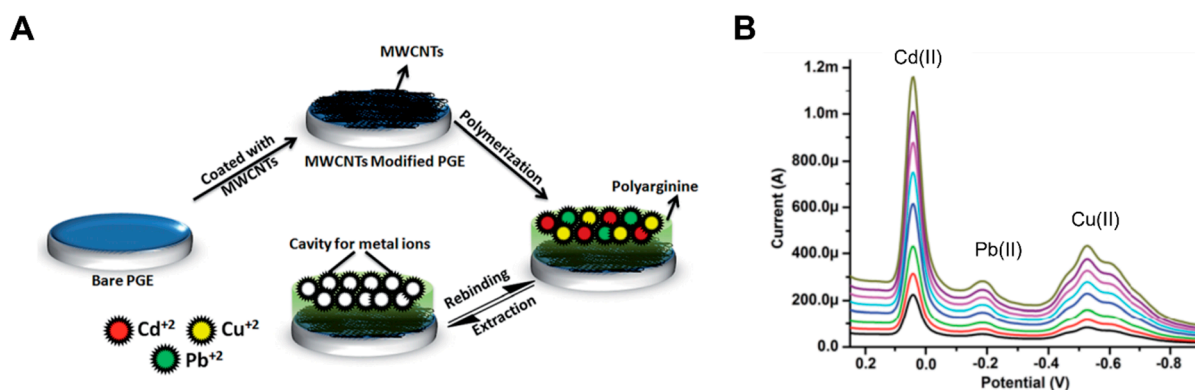


**Figure 5.** (A) Schematic representation showing the production of an imprinted nanowire modified pencil graphite electrode (PGE). (B) Differential pulse stripping voltammograms for the simultaneous detection of cadmium(II), lead(II), and copper(II) at different concentrations. Figure reproduced and modified from [100] with permission from copyright The Royal Society of Chemistry 2014.

### 3.2. Electrochemical Sensors Produced via Screen-Printing

The development and optimization of screen-printed electrodes (SPEs) as the transducer within electroanalytical platforms has further enhanced their intrigue for in-the-field sensing applications due to their high reproducibility, sensitivity, cost effectiveness, and suitability for mass production [101]. Screen-printing as an electrode production method involves the application of a thixotropic fluid through a mesh, which defines the desired size and shape of the electrode. As such, the mesh screens used for the process can be manipulated and designed to form an almost limitless variety of electrode shapes and sizes on various substrates, making them suitable for any application or device [102,103]. It is noted that if a shorter connection length of SPE is used, an improved electrochemical response is obtained [104]. In addition to versatility in the shape and size of the electrode dimensions, there are a wide range of possibilities in manipulation of the ink composition. For example, they can be designed to include a variety of substances including graphene, graphite, and carbon black alongside the binder and solvents [105]. Due to this versatility, there are many examples in the literature of their use as transducers for the monitoring of environmental pollution with a particular focus on the detection of heavy metal ions [49,106–108].

The favorable properties of MIPs, including their chemical/thermal stability, versatility, and suitability for mass production mean they synergize well as recognition elements in conjunction with SPEs. This has been shown for a wide range of analytical systems for the detection of antibiotics [109], neurotransmitters [110], proteins [111], and even microbiological cells [112]. The chemical and thermal stability of MIPs mean that they can be incorporated into SPE platforms in a variety of ways such as non-covalent immobilization [113], covalent attachment [114,115], direct incorporation into the conductive ink [116], or via the formation of the MIP directly onto the surface through electropolymerization [117]. The plethora of MIP synthesis methodologies and incorporation techniques onto SPEs show their suitability for environmental monitoring. Therefore, we expect that the first commercial MIP-based sensors will have SPEs as base electrodes.

#### 4. MIP-Based Optical Assays

One of the most unambiguous approaches in MIP-based sensing is the ability to translate a binding event at the MIP's surface into an optical output. This output can be the result of various molecular mechanisms, (e.g., fluorescence quenching/enhancement, dye displacement, conformation changes, redox reactions) that offer a clear confirmation of a target's presence either by spectroscopic methods or visual observation (Table 5) [14,118–121].

**Table 5.** Summary of studies which have utilized MIPs for the optical detection of various targets.

Target/Synthesis <sup>a</sup>	Sensor Material <sup>b</sup>	Detection Method <sup>c</sup>	Dynamic Concentration Range	LoD	Samples	Ref.
-Cd(II) -RAFT polymerization	MIP-paper composite	Colorimetric	1–100 ng·mL <sup>-1</sup>	0.4 ng·mL <sup>-1</sup>	-Lake/river/tap H <sub>2</sub> O	[122]
-Various psychoactive substances -Bulk polymerization	Dye loaded MIPs	Colorimetric	0.01–0.1 mM	50 μM	-Distilled H <sub>2</sub> O	[123]
-Cartap -Free radical polymerization	Silver nanoparticle sensor with magnetic MIPs	UV-Vis	0.01–30 mg·mL <sup>-1</sup>	10 μg·mL <sup>-1</sup>	-Tea	[124]
-Atrazine -Bulk polymerization	MIP/gold nanoparticle assay	SERS	0.005–1 mg·L <sup>-1</sup>	0.0012 mg·L <sup>-1</sup>	-Apple juice	[125]
-BPA -Bulk polymerization	Paper-based assay with magnetic MIPs	Colorimetric	10–1000 nM	6.18 nM	-Buffered solutions	[126]
-Goesmin -Bulk polymerization	Fluorescent tagged MIPs	Fluorescence	-	80 μg·L <sup>-1</sup>	-Field H <sub>2</sub> O	[127]
-2,4-D -RAFT polymerization	Fluorescent tagged MIPs	Fluorescence	20 nM–5 μM	28 nM	-Field H <sub>2</sub> O from various locations	[128]
-λ-cyhalothrin -Free radical polymerization	MIPs with core-shell QDs	Fluorescence	1–350 μg·g <sup>-1</sup>	0.246 μg·g <sup>-1</sup>	-Various food samples	[129]
-Dichlorophenoxyacetic acid -Bulk polymerization	Paper chip with MIPs and QDs.	Fluorescence	0.51–80 μMol·L <sup>-1</sup>	0.17 μMol·L <sup>-1</sup>	-Cucumber samples	[130]
-Triazophos -Bulk polymerization	MIP-based LFA	Fluorescence	20–500 μg·L <sup>-1</sup>	20 μg·L <sup>-1</sup>	-Tap H <sub>2</sub> O	[131]

<sup>a</sup> Reversible addition–fragmentation chain transfer (RAFT); bisphenol A (BPA); dichlorophenoxyacetic acid (2,4-D).

<sup>b</sup> Quantum dots (QDs); lateral flow assay (LFA). <sup>c</sup> Surface-enhanced Raman spectroscopy (SERS).

##### 4.1. Colorimetric MIP-Based Sensing

The most straightforward approach in MIP-based colorimetric sensing consists of loading an extracted MIP with a visually observable competitor molecule. This can be either the dye-conjugated template or a structurally similar molecule. When the dye-loaded MIP particles are exposed to a solution containing the target molecule, it will bind to the MIP and displace the dye into the surrounding medium. This leads to an observable color reaction confirming the presence of the target. McNiven et al. [132] introduced the first colorimetric MIP displacement assay in 1998, utilizing a dye-conjugated chloramphenicol analog for the detection of the parent chloramphenicol compound. The developed assay demonstrated the selective nature of MIPs, overcoming common interferences whilst also exhibiting a good linear range (within, above, and below the physiological range).

Following this proof-of-principle by McNiven et al. [132], the concept was extended towards the detection of a wide range of compounds, including chlorophenolic contaminants [133], L-phenylalaninamide [134], various amines [135], and drug molecules [123,136]. These studies verified that the methodology could be successfully tailored toward a multitude of targets. In terms of monitoring environmental pollution, a study by Silverio et al. [137] in 2017 demonstrated that it is possible to detect pesticides using MIPs that were pre-loaded with a commercial pH indicator (bromocresol green). The combination of a widely available dye and low-cost MIP system makes this approach commercially very interesting. However, drawbacks are that the study makes use of a UV-Vis spectrophotometer and incubates the samples for over an hour in acetonitrile. A paper by Lowdon et al. [123] demonstrated that it is possible to use a similar system in an aqueous environment and achieve a visible confirmation regarding the target's presence in minutes by immobilizing the dye-loaded MIPs into a syringe filter. This indicates that displacement assays have significant potential for environmental screening as combining such an assay with a low-cost handheld absorption meter would allow an end-user to rapidly detect the presence of various targets, (e.g., pesticides) in liquid environmental samples.

In addition to displacement assays, other MIP-based colorimetric assays have been developed for the detection of environmental pollutants. Huang et al. [122] created polymer-paper composite chips for the colorimetric detection of cadmium ions, for instance. Other assays make use of nanoparticles to catalyze a color reaction in the presence of the target. Typically, MIPs are used to extract compounds from an aqueous solution and are then transferred to a solution containing gold nanoparticles. Elution of the target compound from the MIPs leads to a color change of the solution by interaction of the compound with the nanoparticles. This mechanism was used for the detection of the insecticide cartap [124] and the herbicide atrazine [125]. The drawback of this procedure is that it typically requires a multi-step approach with several reagents employed, making it less suitable for handheld, routine environmental screening. However, Kong et al. [126] used this approach to create a paper-based handheld test strip for the endocrine disruptor BPA. They used cellulose paper on which they created a wax-like scaffold for immobilizing an acrylamide (AA)-based MIP membrane impregnated with silver nanoparticles using EDGMA and benzoin ethyl ether (BEE) as cross-linker and initiator, respectively (Figure 6). A second cellulose paper containing tetramethylbenzidine (TMB) was attached to the first paper. Solutions containing different amounts of BPA were mixed with peroxide and the paper was dipped into this mixture. Without the target molecule present, the interaction of peroxide and nanoparticles led to a blue coloring of the paper. The presence of BPA in the solution prevented this interaction from occurring, leaving the paper indicator uncolored. The color reaction was studied by taking pictures of the paper strip with a simple smartphone camera and analyzing the color intensity using Photoshop. These results illustrate how close this technology is to actual implementation in the field using handheld integrated sensor devices and paper-based dipsticks.

#### 4.2. MIP-Based Fluorescent Detection Assays

Colorimetric detection platforms are interesting from an application point-of-view due to their simple nature and the minimal post-processing of the detection signal. However, the sensitivity of the resulting platforms is usually limited in comparison to similar platforms employing fluorescent dyes. Subsequently, multiple displacement protocols have been developed over the years for the detection of various environmentally significant compounds, such as herbicides [138] and algal metabolites [127]. In addition, it is also possible to fluorescently modify the monomers themselves and incorporate fluorescence into the MIPs directly. Modification of the MIP itself holds some value over the modification of binding molecules as the primary optical transducer is situated in the polymeric network of the receptor. This has the distinct advantage of allowing the MIP to retain the optical property that has been introduced, as well as adding to the reusability of the polymer compared to chromophore/fluorophore-target-conjugates that are lost after bind-



ing. Varying approaches have shown differing success at integrating fluorophores into the structures of MIPs with traditional approaches focusing on the installation of fluorescent functional monomers, cross-linkers, and initiator molecules [139–142]. A urea-expressing fluorescent probe cross-linker that was incorporated into submicron-sized silica particles by Wagner et al. [128] is a prime example of fluorophores in MIP-based systems. The fluorescent MIP shell of the silica was proven to “light up” upon the binding of the carboxylate group present in the herbicide 2,4-D (Figure 7), shifting the observable color of the sensor from yellow to red. The developed assays showed good sensitivity (order of nM), reporting the concentrations of 2,4-D in contaminated water samples and meeting WHO requirements for the analysis of drinking water with a linear range between 20 nM and 5  $\mu$ M [61].

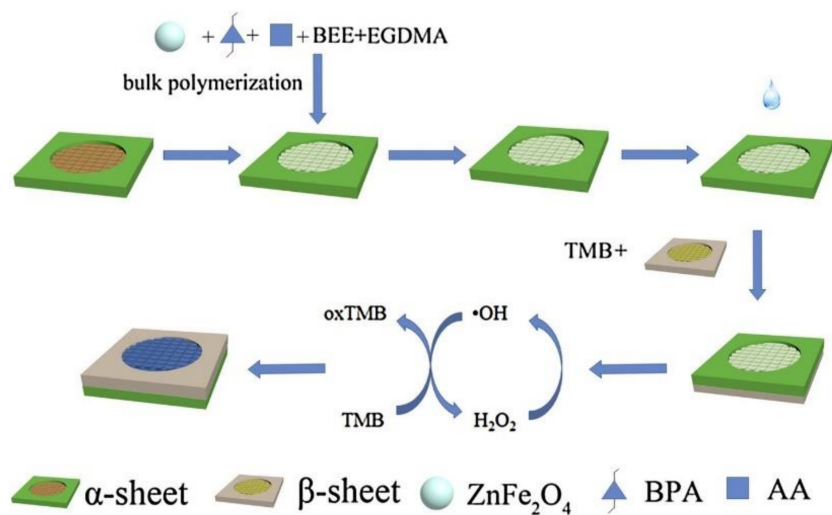


**Figure 6.** Construction of a paper-based MIP assay for the detection of BPA in liquid. Figure reproduced from [126] with permission from copyright Elsevier 2017.

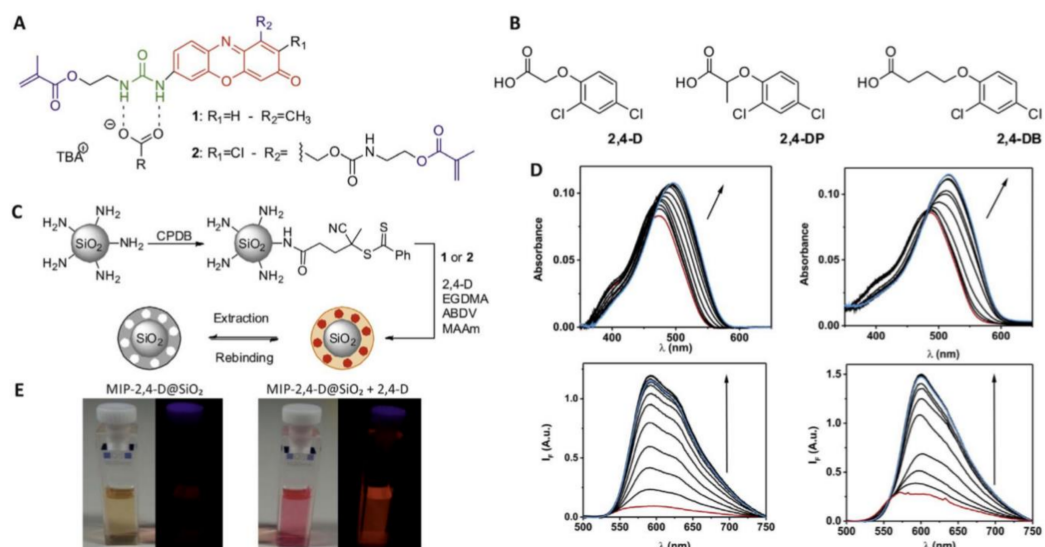


**Figure 7.** (A) Molecular architectures of the phenoxazinone monomer (1) and crosslinker (2). (B) Structures of 2,4-D and closely related compounds 2,4-DP and 2,4-DB. (C) Preparation of the core-shell microparticles from amine-modified silica microparticles with imprinting of the template into the MIP shell, followed by extraction (rebinding = analytical reaction). (D) Absorption and emission of (1) (left) and (2) (right) upon addition of 2,4-D/tertiary butyl alcohol (TBA) in CHCl<sub>3</sub> ([1]=[2] = 5  $\mu$ M, [2,4-D]/[TBA] = 0–250  $\mu$ M). (E) Photographs of (2) in CHCl<sub>3</sub> in the absence (left) and presence (right) of 2,4-D/TBA in daylight and under UV lamp (365 nm) illumination. Figure reproduced from [128] with permission from copyright Elsevier 2018.

An alternative approach to achieving fluorescent characteristics in MIPs has been the introduction of nanoparticles, in particular QDs. Installation of core-shell QDs that are synthesized from various metals/carbon (typically Mn, Cu, Zn, or C) allow emitted wavelengths to be tailored towards a desired application [143–145]. The surrounding MIP layer remains thin, which enables the emission of wavelengths when no target is bound to the cavities. However, once target molecules are bound to the cavities, the emission is blocked. Wei et al. [129] exemplified this technology by introducing a core-shell QD MIP-based fluorescent sensor engineered towards the detection of  $\lambda$ -cyhalothrin (a common pesticide). The sensory device showed a linear decrease in fluorescence in the presence of  $\lambda$ -cyhalothrin with a linear range and LoD of 1–350 and  $0.246 \mu\text{g}\cdot\text{g}^{-1}$ , respectively. Combining this MIP-based QD technology with microfluidics and biodegradable substrates enables the prospect for rapid handheld analysis of samples. Hao et al. [130] explored this concept by generating an imprinted paper chip-based fluorescent assay for the detection of 2,4-D (Figure 8). Cadmium telluride QDs were utilized in conjunction with rhodamine B (RhB) for the dual emission detection of the herbicide. These QDs were installed into the porous paper matrix, while retaining the ability to emit stimulated fluorescence. The use of the paper substrate allows the developed device to remain cheap and offers the potential for reusability as the paper-based substrate is easily exchanged. Although these innovations are promising, the LoD and linear range of the device suffers with a  $\mu\text{M}$  range only being explored in the research.

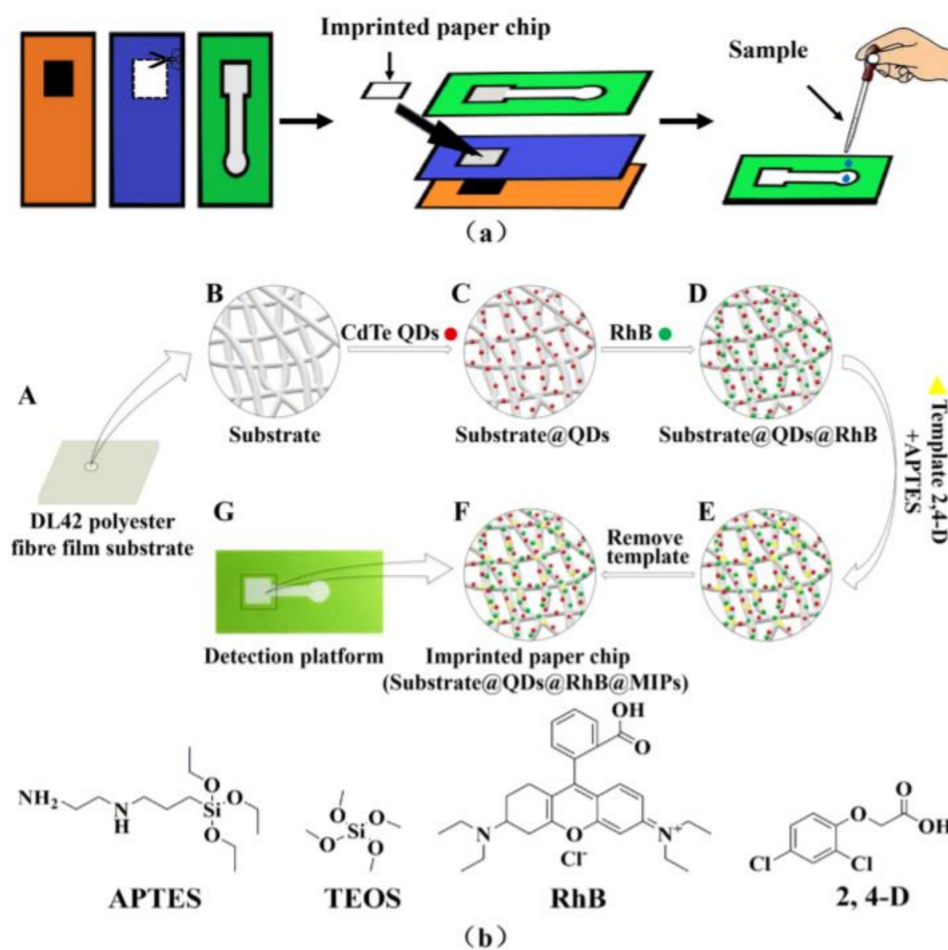


**Figure 8.** (a) Assembly of imprinted paper chip. (b) Synthesis diagram of detection platform where A is the DL42 substrate, B–F is the preparation process of the imprinted paper chip, and G is the prepared product installed on the substrate. The chemical structures of 3-aminopropyltriethoxysilane (APTES), tetraethyl orthosilicate (TEOS), RhB, and 2,4-D are also included. Figure reproduced from [130] with permission from copyright Elsevier 2020.

Finally, MIPs can also be used as antibody analogs in ELISA-like pseudo-immunoassays. These assays benefit from the rapid technological progression in the field of ELISA assays. He et al. [131] demonstrated how MIPs can be used to replace the capture antibody in a LFA. Cellulose acetate layers were immobilized on the test line of a typical dipstick and were imprinted with the pesticide triazophos. Samples under study were introduced on a sample pad from which they were transported by capillary forces to the absorbent pad of the stick via the MIP layer. Tap water samples were mixed with a solution containing triazophos-IgG-conjugates. At the test line, these fluorescent conjugates will bind to the MIPs but since the MIPs have a higher affinity for the free version of the pesticide, any trace amount of triazophos will result in less conjugate binding and a more intense color signal in the read-out pad of the stick. The combination of MIP-based LFAs and handheld absorption meters may potentially result in the development of handheld pesticide detection kits for environmental monitoring in the coming years.

#### 4.3. Other Optical MIP-Based Sensors

Many sensor platforms, especially those developed for the specific detection of ions and heavy metals, are based on more complex optical detection platforms such as surface plasmon resonance, photonic crystals, or flame atomic absorption spectroscopy [146–148]. Last year, Meza Lopéz et al. [149] introduced a highly applied sensor platform for the detection of lead ions in real water samples. They coated optical fibers with 2-acrylamido-2-methylpropane sulfonic acid-based surface imprinted polymers. The resulting optical fiber was coupled to a spectrophotometer for the optical detection of lead ions at ultra-low concentrations (LoD of  $85 \text{ ng L}^{-1}$ ) with selectivity factors for other metal ions ranging from 10 to 40. A promising optical method for micropollutant detection is graphene-mediated surface-enhanced Raman scattering (GERS). For example, Carboni et al. [150] utilized molecularly imprinted GERS materials for the detection of the organophosphate paraoxon. The results demonstrated a sensitive and highly specific detection of the toxic organic pollutant.

### 5. Future MIP-Based Sensors

A recent breakthrough in nanotechnology relating to MIPs is the development of MIP-aptamer hybrid systems, which are likely to improve overall MIP performance and therefore facilitate commercial adoption. These composites have shown enhanced stability, and in some cases, also affinity [10]. “AptaMIPs” are typically made by first producing a polymerizable version of an aptamer and then incorporating the polymerizable aptamer into the typical monomeric mixture employed in the imprinting process. Based on this concept, Turner et al. [151] developed a hybrid affinity reagent for the recognition of the antibiotic moxifloxacin, achieving a 10-fold superior binding performance over conventional nanoMIPs, with the lowest  $K_D$  values reported at 3.65 nM. However, given the very recent nature of this novel hybrid technology, its optimization phase is still in progress. For example, the identity and length of the linker used in generating the polymerizable aptamer, as well as its position within the aptamer are yet to be investigated. A comprehensive review article has recently been published and summarizes the main production techniques of such AptaMIPs together with their application for the detection of environmental pollutants, proteins, metals, explosives, viruses, and pharmaceuticals [152].

### 6. Outlook

MIPs are cost-effective, highly selective, and robust affinity ligands which makes them excellent candidates for the determination and quantification of heavy metals and pollutants in diagnostically challenging (extreme of pH and temperature) environments. In this review, we have focused on MIPs using electrochemical and optical transduction for determination of heavy metals and pollutants since these methods have the highest promise for integration into portable devices. Although there is an exponential increase in the number of publications related to electrochemical and optical MIP-based sensors for

various targets, their development for future commercial applications must be improved. Particularly, their affinity to the target upon exposure to real or complex matrices and the development of array formats. It is clear that nanomaterials significantly improve the analytical performance of MIP-based sensors, although their synthesis protocol should be kept simple and compatible with mass production. After a comprehensive literature review of MIP-based sensors, it appears that their implementation using electrochemical detection is the most promising for commercial applications due to its high specificity, inherent simplicity, and low-cost components. Screen-printing is a preferential approach due to its cost-effectiveness in terms of large-scale sensor production. In applications where high sensitivity is not required, colorimetric detection might be preferred due to the easy interpretation and limited post-processing required. These platforms are particularly suitable for in-field testing in areas with limited resources or where high-throughput of samples is required. In the coming years, breakthroughs in nanotechnology and integration of MIPs into mass-producible sensors, such as via screen-printing technology, will pave the way for the commercial applications of MIP-based sensors.

**Author Contributions:** Conceptualization, M.P. and J.M.; writing – original draft preparation, P.M.S.T., R.D.C., K.E., J.W.L., K.B., U.R., F.C. and J.M.; Writing – review and editing, F.C., M.P. and J.M.; Supervision, C.E.B., B.v.G. and M.P. All authors have read and agreed to the published version of the manuscript.

**Funding:** P.M.S.T. would like to thank the Royal Society of Chemistry for the Researcher Mobility Grant (M19-7489). U.R. thanks the country of Lower Austria for financial support (Project number WST3-F-5030820/012-2019).

**Institutional Review Board Statement:** Not applicable.

**Informed Consent Statement:** Not applicable.

**Data Availability Statement:** Not applicable.

**Conflicts of Interest:** The authors declare no conflict of interest.

## References

1. Berglund, L.; Björling, E.; Oksvold, P.; Fagerberg, L.; Asplund, A.; Szigyarto, C.A.-K.; Persson, A.; Ottosson, J.; Wernérus, H.; Nilsson, P.; et al. A Genecentric Human Protein Atlas for Expression Profiles Based on Antibodies. *Mol. Cell. Proteom.* **2008**, *7*, 2019–2027. [[CrossRef](#)] [[PubMed](#)]
2. Gray, A.C.; Bradbury, A.R.M.; Knappik, A.; Plückthun, A.; Borrebaeck, C.A.K.; Dübel, S. Animal-derived-antibody generation faces strict reform in accordance with European Union policy on animal use. *Nat. Methods* **2020**, *17*, 755–756. [[CrossRef](#)] [[PubMed](#)]
3. Ahlgren, S.; Wällberg, H.; Tran, T.A.; Widström, C.; Hjertman, M.; Abrahamsén, L.; Berndorff, D.; Dinkelborg, L.M.; Cyr, J.E.; Feldwisch, J.; et al. Targeting of HER2-Expressing Tumors with a Site-Specifically <sup>99m</sup>Tc-Labeled Recombinant Affibody Molecule, ZHER2:2395, with C-Terminally Engineered Cysteine. *J. Nucl. Med.* **2009**, *50*, 781–789. [[CrossRef](#)] [[PubMed](#)]
4. Barozzi, A.; Lavoie, R.A.; Day, K.N.; Prodromou, R.; Menegatti, S. Affibody-Binding Ligands. *Int. J. Mol. Sci.* **2020**, *21*, 3769. [[CrossRef](#)] [[PubMed](#)]
5. Satheeshkumar, P.K. Expression of Single Chain Variable Fragment (scFv) Molecules in Plants: A Comprehensive Update. *Mol. Biotechnol.* **2020**, *62*, 151–167. [[CrossRef](#)]
6. Crivianu-Gaita, V.; Thompson, M. Aptamers, Antibody ScFv, and Antibody Fab' Fragments: An Overview and Comparison of Three of the Most Versatile Biosensor Biorecognition Elements. *Biosens. Bioelectron.* **2016**, *85*, 32–45. [[CrossRef](#)]
7. Jayasena, S.D. Aptamers: An Emerging Class of Molecules That Rival Antibodies in Diagnostics. *Clin. Chem.* **1999**, *45*, 1628–1650. [[CrossRef](#)] [[PubMed](#)]
8. Zhang, Y.; Lai, B.S.; Juhas, M. Recent Advances in Aptamer Discovery and Applications. *Molecules* **2019**, *24*, 941. [[CrossRef](#)]
9. Keum, J.-W.; Bermudez, H. Enhanced resistance of DNA nanostructures to enzymatic digestion. *Chem. Commun.* **2009**, 7036–7038. [[CrossRef](#)] [[PubMed](#)]
10. Poma, A.; Brahmabhatt, H.; Pendergraft, H.M.; Watts, J.K.; Turner, N.W. Generation of Novel Hybrid Aptamer-Molecularly Imprinted Polymeric Nanoparticles. *Adv. Mater.* **2015**, *27*, 750–758. [[CrossRef](#)]
11. Jolly, P.; Tamboli, V.; Harniman, R.L.; Estrela, P.; Allender, C.J.; Bowen, J.L. Aptamer–MIP hybrid receptor for highly sensitive electrochemical detection of prostate specific antigen. *Biosens. Bioelectron.* **2016**, *75*, 188–195. [[CrossRef](#)] [[PubMed](#)]
12. Menger, M.; Yarman, A.; Erdössy, J.; Yildiz, H.B.; Gyurcsányi, R.E.; Scheller, F.W. MIPs and Aptamers for Recognition of Proteins in Biomimetic Sensing. *Biosensors* **2016**, *6*, 35. [[CrossRef](#)] [[PubMed](#)]



13. Canfarotta, F.; Poma, A.; Guerreiro, A.; Piletsky, S. Solid-phase synthesis of molecularly imprinted nanoparticles. *Nat. Protoc.* **2016**, *11*, 443–455. [[CrossRef](#)] [[PubMed](#)]
14. Lowdon, J.W.; Diliën, H.; Singla, P.; Peeters, M.; Cleij, T.J.; van Grinsven, B.; Eersels, K. MIPs for commercial application in low-cost sensors and assays—An overview of the current status quo. *Sens. Actuators B Chem.* **2020**, *325*, 128973. [[CrossRef](#)] [[PubMed](#)]
15. Lorenzo, R.A.; Carro, A.M.; Alvarez-Lorenzo, C.; Concheiro, A. To Remove or Not to Remove? The Challenge of Extracting the Template to Make the Cavities Available in Molecularly Imprinted Polymers (MIPs). *Int. J. Mol. Sci.* **2011**, *12*, 4327–4347. [[CrossRef](#)] [[PubMed](#)]
16. Vasapollo, G.; Del Sole, R.; Mergola, L.; Lazzoi, M.R.; Scardino, A.; Scorrano, S.; Mele, G. Molecularly Imprinted Polymers: Present and Future Prospective. *Int. J. Mol. Sci.* **2011**, *12*, 5908–5945. [[CrossRef](#)]
17. Fischer, E. Influence of Configuration on the Action of Enzymes. *J. Am. Chem. Soc.* **1894**, *3*, 2985–2993. [[CrossRef](#)]
18. Alexander, C.; Andersson, H.; Andersson, L.I.; Ansell, R.J.; Kirsch, N.; Nicholls, I.A.; O'Mahony, J.; Whitcombe, M.J. Molecular imprinting science and technology: A survey of the literature for the years up to and including 2003. *J. Mol. Recognit.* **2006**, *19*, 106–180. [[CrossRef](#)] [[PubMed](#)]
19. Polyakov, M.V. Adsorption Properties and Structure of Silica Gel. *Zhurnal Fizicheskoi Khimii/Akad. SSSR* **1931**, *2*, 799–805.
20. Dickey, F.H. The Preparation of Specific Adsorbents. *Proc. Natl. Acad. Sci. USA* **1949**, *35*, 227–229. [[CrossRef](#)]
21. O'Mahony, J.; Karlsson, B.C.G.; Mizaikoff, B.; Nicholls, I.A. Correlated theoretical, spectroscopic and X-ray crystallographic studies of a non-covalent molecularly imprinted polymerisation system. *Analyst* **2007**, *132*, 1161–1168. [[CrossRef](#)] [[PubMed](#)]
22. Lai, J.-P.; Yang, M.-L.; Niessner, R.; Knopp, D. Molecularly imprinted microspheres and nanospheres for di(2-ethylhexyl)phthalate prepared by precipitation polymerization. *Anal. Bioanal. Chem.* **2007**, *389*, 405–412. [[CrossRef](#)] [[PubMed](#)]
23. Sellergren, B.; Lepistö, M.; Mosbach, K. Highly Enantioselective and Substrate-Selective Polymers Obtained by Molecular Imprinting Utilizing Noncovalent Interactions. NMR and Chromatographic Studies on the Nature of Recognition. *J. Am. Chem. Soc.* **1988**, *110*, 5853–5860. [[CrossRef](#)]
24. Wulff, G.; Heide, B.; Helfmeier, G. Enzyme-analog built polymers. 20. Molecular recognition through the exact placement of functional groups on rigid matrixes via a template approach. *J. Am. Chem. Soc.* **1986**, *108*, 1089–1091. [[CrossRef](#)]
25. Balasubramanian, S.; Rani, B.A. Computational and Experimental Studies of Molecularly Imprinted Polymers for Organochlorine Pesticides Heptachlor and DDT. *Curr. Anal. Chem.* **2012**, *8*, 562–568. [[CrossRef](#)]
26. Cowen, T.; Karim, K.; Piletsky, S. Computational approaches in the design of synthetic receptors—A review. *Anal. Chim. Acta* **2016**, *936*, 62–74. [[CrossRef](#)]
27. Piletsky, S.A.; Karim, K.; Piletska, E.V.; Day, C.J.; Freebairn, K.W.; Legge, C.; Turner, A.P.F. Recognition of ephedrine enantiomers by molecularly imprinted polymers designed using a computational approach. *Analyst* **2001**, *126*, 1826–1830. [[CrossRef](#)]
28. Madikizela, L.M.; Tavengwa, N.T.; Tutu, H.; Chimuka, L. Green aspects in molecular imprinting technology: From design to environmental applications. *Trends Environ. Anal. Chem.* **2018**, *17*, 14–22. [[CrossRef](#)]
29. Poma, A.; Turner, A.P.; Piletsky, S.A. Advances in the manufacture of MIP nanoparticles. *Trends Biotechnol.* **2010**, *28*, 629–637. [[CrossRef](#)]
30. Ye, L.; Cormack, P.A.G.; Mosbach, K. Molecularly imprinted monodisperse microspheres for competitive radioassay. *Anal. Commun.* **1999**, *36*, 35–38. [[CrossRef](#)]
31. Vaihinger, D.; Landfester, K.; Kräuter, I.; Brunner, H.; Tovar, G.E.M. Molecularly Imprinted Polymer Nanospheres as Synthetic Affinity Receptors Obtained by Miniemulsion Polymerisation. *Macromol. Chem. Phys.* **2002**, *203*, 1965–1973. [[CrossRef](#)]
32. Moral, N.P.; Mayes, A.G. Molecular Imprinting of Polymeric Core-Shell Nanoparticles. *MRS Online Proc. Libr.* **2002**, *723*. [[CrossRef](#)]
33. Tan, C.J.; Tong, Y.W. Molecularly imprinted beads by surface imprinting. *Anal. Bioanal. Chem.* **2007**, *389*, 369–376. [[CrossRef](#)] [[PubMed](#)]
34. Carboni, D.; Flavin, K.; Servant, A.; Gouverneur, V.; Resmini, M. The First Example of Molecularly Imprinted Nanogels with Aldolase Type I Activity. *Chem. A Eur. J.* **2008**, *14*, 7059–7065. [[CrossRef](#)]
35. Piletsky, S.; Piletska, E.; Sergeeva, T.A.; Nicholls, I.A.; Weston, D.; Turner, A. Synthesis of biologically active molecules by imprinting polymerisation. *Biopolym. Cell* **2006**, *22*, 63–67. [[CrossRef](#)]
36. Nematollahzadeh, A.; Sun, W.; Aureliano, C.S.A.; Lütkemeyer, D.; Stute, J.; Abdekhodaie, M.J.; Shojaei, A.; Sellergren, B. High-Capacity Hierarchically Imprinted Polymer Beads for Protein Recognition and Capture. *Angew. Chem. Int. Ed.* **2011**, *50*, 495–498. [[CrossRef](#)]
37. Dickert, F.L.; Hayden, O.; Halikias, K.P. Synthetic receptors as sensor coatings for molecules and living cells. *Analyst* **2001**, *126*, 766–771. [[CrossRef](#)] [[PubMed](#)]
38. Schirhagl, R.; Ren, K.; Zare, R.N. Surface-imprinted polymers in microfluidic devices. *Sci. China Ser. B Chem.* **2012**, *55*, 469–483. [[CrossRef](#)]
39. de Castro, M.L.; Priego-Capote, F. Soxhlet extraction: Past and present panacea. *J. Chromatogr. A* **2010**, *1217*, 2383–2389. [[CrossRef](#)]
40. Luque-García, J.; de Castro, M.L. Ultrasound: A powerful tool for leaching. *TrAC Trends Anal. Chem.* **2003**, *22*, 41–47. [[CrossRef](#)]
41. Tobiszewski, M.; Mechlińska, A.; Zygmunt, B.; Namiesnik, J. Green analytical chemistry in sample preparation for determination of trace organic pollutants. *TrAC Trends Anal. Chem.* **2009**, *28*, 943–951. [[CrossRef](#)]



42. Ertürk, G.; Berillo, D.; Hedström, M.; Mattiasson, B. Microcontact-BSA imprinted capacitive biosensor for real-time, sensitive and selective detection of BSA. *Biotechnol. Rep.* **2014**, *3*, 65–72. [[CrossRef](#)] [[PubMed](#)]
43. Rebocho, S.; Cordas, C.M.; Viveiros, R.; Casimiro, T. Development of a ferrocenyl-based MIP in supercritical carbon dioxide: Towards an electrochemical sensor for bisphenol A. *J. Supercrit. Fluids* **2018**, *135*, 98–104. [[CrossRef](#)]
44. Liu, Z.; Xu, Z.; Wang, D.; Yang, Y.; Duan, Y.; Ma, L.; Lin, T.; Liu, H. A Review on Molecularly Imprinted Polymers Preparation by Computational Simulation-Aided Methods. *Polymers* **2021**, *13*, 2657. [[CrossRef](#)]
45. Turiel, E.; Martín-Esteban, A. Molecularly imprinted polymers for sample preparation: A review. *Anal. Chim. Acta* **2010**, *668*, 87–99. [[CrossRef](#)]
46. Yarman, A.; Scheller, F.W. How Reliable Is the Electrochemical Readout of MIP Sensors? *Sensors* **2020**, *20*, 2677. [[CrossRef](#)]
47. Tchounwou, P.B.; Yedjou, C.G.; Patlolla, A.K.; Sutton, D.J. Heavy metal toxicity and the environment. *Mol. Clin. Environ. Toxicol.* **2012**, *101*, 133–164. [[CrossRef](#)]
48. Briffa, J.; Sinagra, E.; Blundell, R. Heavy metal pollution in the environment and their toxicological effects on humans. *Heliyon* **2020**, *6*, e04691. [[CrossRef](#)]
49. Ferrari, A.G.-M.; Carrington, P.; Rowley-Neale, S.J.; Banks, C.E. Recent advances in portable heavy metal electrochemical sensing platforms. *Environ. Sci. Water Res. Technol.* **2020**, *6*, 2676–2690. [[CrossRef](#)]
50. European Parliament. *Council Directive 98/83/EC of 3 November 1998 on the Quality of Water Intended for Human Consumption*; European Parliament: Strasbourg, France, 2020.
51. Pohl, P. Determination of metal content in honey by atomic absorption and emission spectrometries. *TrAC Trends Anal. Chem.* **2009**, *28*, 117–128. [[CrossRef](#)]
52. Flamini, R.; Panighel, A. Mass spectrometry in grape and wine chemistry. Part II: The consumer protection. *Mass Spectrom. Rev.* **2006**, *25*, 741–774. [[CrossRef](#)] [[PubMed](#)]
53. Peng, G.; He, Q.; Zhou, G.; Li, Y.; Su, X.; Liu, M.; Fan, L. Determination of heavy metals in water samples using dual-cloud point extraction coupled with inductively coupled plasma mass spectrometry. *Anal. Methods* **2015**, *7*, 6732–6739. [[CrossRef](#)]
54. Byers, H.L.; McHenry, L.J.; Grundl, T.J. XRF techniques to quantify heavy metals in vegetables at low detection limits. *Food Chem. X* **2019**, *1*, 100001. [[CrossRef](#)]
55. Oehme, I.; Wolfbeis, O.S. Optical sensors for determination of heavy metal ions. *Mikrochim. Acta* **1997**, *126*, 177–192. [[CrossRef](#)]
56. Soylak, M.; Aydin, A. Determination of some heavy metals in food and environmental samples by flame atomic absorption spectrometry after coprecipitation. *Food Chem. Toxicol.* **2011**, *49*, 1242–1248. [[CrossRef](#)]
57. Nishide, H.; Deguchi, J.; Tsuchida, E. Selective Adsorption of Metal Ions on Crosslinked Poly(Vinylpyridine) Resin Prepared With a Metal Ion As a Template. *Chem. Lett.* **1976**, *5*, 169–174. [[CrossRef](#)]
58. Branger, C.; Meouche, W.; Margailan, A. Recent advances on ion-imprinted polymers. *React. Funct. Polym.* **2013**, *73*, 859–875. [[CrossRef](#)]
59. Wani, A.L.; Ara, A.; Usmani, J.A. Lead toxicity: A review. *Interdiscip. Toxicol.* **2015**, *8*, 55–64. [[CrossRef](#)]
60. Lanphear, B.P.; Hornung, R.; Khoury, J.; Yolton, K.; Baghurst, P.; Bellinger, D.C.; Canfield, R.L.; Dietrich, K.N.; Bornschein, R.; Greene, T.; et al. Low-Level Environmental Lead Exposure and Children’s Intellectual Function: An International Pooled Analysis. *Environ. Health Perspect.* **2005**, *113*, 894–899. [[CrossRef](#)] [[PubMed](#)]
61. World Health Organization. *Guidelines for Drinking-Water Quality: Fourth Edition Incorporating First Addendum*; World Health Organization: Geneva, Switzerland, 2017.
62. Alizadeh, T.; Amjadi, S. Preparation of nano-sized Pb<sup>2+</sup> imprinted polymer and its application as the chemical interface of an electrochemical sensor for toxic lead determination in different real samples. *J. Hazard. Mater.* **2011**, *190*, 451–459. [[CrossRef](#)]
63. Bojdi, M.K.; Mashhadizadeh, M.H.; Behbahani, M.; Farahani, A.; Davarani, S.S.H.; Bagheri, A. Synthesis, characterization and application of novel lead imprinted polymer nanoparticles as a high selective electrochemical sensor for ultra-trace determination of lead ions in complex matrixes. *Electrochim. Acta* **2014**, *136*, 59–65. [[CrossRef](#)]
64. Bahrami, A.; Besharati-Seidani, A.; Abbaspour, A.; Shamsipur, M. A highly selective voltammetric sensor for sub-nanomolar detection of lead ions using a carbon paste electrode impregnated with novel ion imprinted polymeric nanobeads. *Electrochim. Acta* **2014**, *118*, 92–99. [[CrossRef](#)]
65. Hu, S.; Xiong, X.; Huang, S.; Lai, X. Preparation of Pb(II) Ion Imprinted Polymer and Its Application as the Interface of an Electrochemical Sensor for Trace Lead Determination. *Anal. Sci.* **2016**, *32*, 975–980. [[CrossRef](#)]
66. Alizadeh, T.; Hamidi, N.; Ganjali, M.R.; Rafiei, F. An extraordinarily sensitive voltammetric sensor with picomolar detection limit for Pb<sup>2+</sup> determination based on carbon paste electrode impregnated with nano-sized imprinted polymer and multi-walled carbon nanotubes. *J. Environ. Chem. Eng.* **2017**, *5*, 4327–4336. [[CrossRef](#)]
67. Luo, X.; Huang, W.; Shi, Q.; Xu, W.; Luan, Y.; Yang, Y.; Wang, H.; Yang, W. Electrochemical sensor based on lead ion-imprinted polymer particles for ultra-trace determination of lead ions in different real samples. *RSC Adv.* **2017**, *7*, 16033–16040. [[CrossRef](#)]
68. Tarley, C.R.T.; Basaglia, A.M.; Segatelli, M.G.; Prete, M.C.; Suquila, F.A.C.; de Oliveira, L.L.G. Preparation and application of nanocomposite based on imprinted poly(methacrylic acid)-PAN/MWCNT as a new electrochemical selective sensing platform of Pb<sup>2+</sup> in water samples. *J. Electroanal. Chem.* **2017**, *801*, 114–121. [[CrossRef](#)]
69. Sebastian, M.; Mathew, B. Ion imprinting approach for the fabrication of an electrochemical sensor and sorbent for lead ions in real samples using modified multiwalled carbon nanotubes. *J. Mater. Sci.* **2018**, *53*, 3557–3572. [[CrossRef](#)]

70. Shamsipur, M.; Samandari, L.; Besharati-Seidani, A.; Pashabadi, A. Synthesis, characterization and using a new terpyridine moiety-based ion-imprinted polymer nanoparticle: Sub-nanomolar detection of Pb(II) in biological and water samples. *Chem. Pap.* **2018**, *72*, 2707–2717. [[CrossRef](#)]
71. Dahaghin, Z.; Kilmartin, P.A.; Mousavi, H.Z. Novel ion imprinted polymer electrochemical sensor for the selective detection of lead(II). *Food Chem.* **2020**, *303*, 125374. [[CrossRef](#)] [[PubMed](#)]
72. Ardalani, M.; Shamsipur, M.; Besharati-Seidani, A. A new generation of highly sensitive potentiometric sensors based on ion imprinted polymeric nanoparticles/multiwall carbon nanotubes/polyaniline/graphite electrode for sub-nanomolar detection of lead(II) ions. *J. Electroanal. Chem.* **2020**, *879*, 114788. [[CrossRef](#)]
73. Bernhoft, R.A. Mercury Toxicity and Treatment: A Review of the Literature. *J. Environ. Public Health* **2012**, *2012*, 460508. [[CrossRef](#)]
74. Martinez-Finley, E.J.; Aschner, M. Recent Advances in Mercury Research. *Curr. Environ. Health Rep.* **2014**, *1*, 163–171. [[CrossRef](#)] [[PubMed](#)]
75. Alizadeh, T.; Ganjali, M.R.; Zare, M. Application of an Hg<sup>2+</sup> selective imprinted polymer as a new modifying agent for the preparation of a novel highly selective and sensitive electrochemical sensor for the determination of ultratrace mercury ions. *Anal. Chim. Acta* **2011**, *689*, 52–59. [[CrossRef](#)] [[PubMed](#)]
76. Rajabi, H.R.; Roushani, M.; Shamsipur, M. Development of a highly selective voltammetric sensor for nanomolar detection of mercury ions using glassy carbon electrode modified with a novel ion imprinted polymeric nanobeads and multi-wall carbon nanotubes. *J. Electroanal. Chem.* **2013**, *693*, 16–22. [[CrossRef](#)]
77. Shirzadmehr, A.; Afkhami, A.; Madrakian, T. A new nano-composite potentiometric sensor containing an Hg<sup>2+</sup>-ion imprinted polymer for the trace determination of mercury ions in different matrices. *J. Mol. Liq.* **2015**, *204*, 227–235. [[CrossRef](#)]
78. Bahrami, A.; Besharati-Seidani, A.; Abbaspour, A.; Shamsipur, M. A highly selective voltammetric sensor for nanomolar detection of mercury ions using a carbon ionic liquid paste electrode impregnated with novel ion imprinted polymeric nanobeads. *Mater. Sci. Eng. C* **2015**, *48*, 205–212. [[CrossRef](#)] [[PubMed](#)]
79. Ghanei-Motlagh, M.; Taher, M.A.; Heydari, A.; Ghanei-Motlagh, R.; Gupta, V.K. A novel voltammetric sensor for sensitive detection of mercury(II) ions using glassy carbon electrode modified with graphene-based ion imprinted polymer. *Mater. Sci. Eng. C* **2016**, *63*, 367–375. [[CrossRef](#)] [[PubMed](#)]
80. Afkhami, A.; Madrakian, T.; Soltani-Shahrivar, M.; Ahmadi, M.; Ghaedi, H. Selective and Sensitive Electrochemical Determination of Trace Amounts of Mercury Ion in Some Real Samples Using an Ion Imprinted Polymer Nano-Modifier. *J. Electrochem. Soc.* **2015**, *163*, B68–B75. [[CrossRef](#)]
81. Alizadeh, T.; Hamidi, N.; Ganjali, M.R.; Rafiei, F. Determination of subnanomolar levels of mercury (II) by using a graphite paste electrode modified with MWCNTs and Hg(II)-imprinted polymer nanoparticles. *Mikrochim. Acta* **2018**, *185*, 16. [[CrossRef](#)] [[PubMed](#)]
82. Velepini, T.; Pillay, K.; Mbianda, X.Y.; Arotiba, O. Application of a Polypyrrole/Carboxy Methyl Cellulose Ion Imprinted Polymer in the Electrochemical Detection of Mercury in Water. *Electroanalysis* **2018**, *30*, 2612–2619. [[CrossRef](#)]
83. Ganjali, M.R.; Rahmani, A.R.; Shokoohi, R.; Farmany, A.; Khazaei, M. A Highly Sensitive and Selective Electrochemical Mercury(II) Sensor Based on Nanoparticles of Hg(II)-Imprinted Polymer and Graphitic Carbon Nitride (g-C<sub>3</sub>N<sub>4</sub>). *Int. J. Electrochem. Sci.* **2019**, *14*, 6420–6430. [[CrossRef](#)]
84. Khazaei, M.; Rahmani, A.R.; Shokoohi, R.; Farmany, A. Development and Application of a Potentiometric Hg<sup>2+</sup>-Imprinted Polymer/Graphitic Carbon Nitride/Carbon Paste Electrode. *Anal. Bioanal. Electrochem.* **2019**, *11*, 535–545.
85. Ait-Touchente, Z.; Sakhraoui, H.E.E.Y.; Fourati, N.; Zerrouki, C.; Maouche, N.; Yaakoubi, N.; Touzani, R.; Chehimi, M.M. High Performance Zinc Oxide Nanorod-Doped Ion Imprinted Polypyrrole for the Selective Electroensing of Mercury II Ions. *Appl. Sci.* **2020**, *10*, 7010. [[CrossRef](#)]
86. Genchi, G.; Sinicropi, M.S.; Lauria, G.; Carocci, A.; Catalano, A. The Effects of Cadmium Toxicity. *Int. J. Environ. Res. Public Health* **2020**, *17*, 3782. [[CrossRef](#)]
87. Alizadeh, T.; Ganjali, M.R.; Nourozi, P.; Zare, M.; Hoseini, M. A carbon paste electrode impregnated with Cd<sup>2+</sup> imprinted polymer as a new and high selective electrochemical sensor for determination of ultra-trace Cd<sup>2+</sup> in water samples. *J. Electroanal. Chem.* **2011**, *657*, 98–106. [[CrossRef](#)]
88. Dahaghin, Z.; Kilmartin, P.A.; Mousavi, H.Z. Determination of cadmium(II) using a glassy carbon electrode modified with a Cd-ion imprinted polymer. *J. Electroanal. Chem.* **2018**, *810*, 185–190. [[CrossRef](#)]
89. Wu, S.; Li, K.; Dai, X.; Zhang, Z.; Ding, F.; Li, S. An ultrasensitive electrochemical platform based on imprinted chitosan/gold nanoparticles/graphene nanocomposite for sensing cadmium (II) ions. *Microchem. J.* **2020**, *155*, 104710. [[CrossRef](#)]
90. Ganjali, H.; Ganjali, M.R.; Alizadeh, T.; Faridbod, F.; Norouzi, P. Bio-Mimetic Cadmium Ion Imprinted Polymer Based Potentiometric Nano-Composite Sensor. *Int. J. Electrochem. Sci.* **2011**, *6*, 6085–6093.
91. Ashkenani, H.; Taher, M.A. Determination of cadmium(II) using carbon paste electrode modified with a Cd-ion imprinted polymer. *Mikrochim. Acta* **2012**, *178*, 53–60. [[CrossRef](#)]
92. Ivari, S.A.R.; Darroudi, A.; Zavar, M.H.A.; Zohuri, G.; Ashraf, N. Ion imprinted polymer based potentiometric sensor for the trace determination of Cadmium (II) ions. *Arab. J. Chem.* **2017**, *10*, S864–S869. [[CrossRef](#)]
93. Coelho, M.K.L.; De Oliveira, H.L.; De Almeida, F.G.; Borges, K.B.; Tarley, C.R.T.; Pereira, A.C. Development of carbon paste electrode modified with cadmium ion-imprinted polymer for selective voltammetric determination of Cd<sup>2+</sup>. *Int. J. Environ. Anal. Chem.* **2017**, *97*, 1378–1392. [[CrossRef](#)]

94. Ghanei-Motlagh, M.; Taher, M. Novel imprinted polymeric nanoparticles prepared by sol–gel technique for electrochemical detection of toxic cadmium(II) ions. *Chem. Eng. J.* **2017**, *327*, 135–141. [[CrossRef](#)]
95. Aravind, A.; Mathew, B. Tailoring of nanostructured material as an electrochemical sensor and sorbent for toxic Cd(II) ions from various real samples. *J. Anal. Sci. Technol.* **2018**, *9*, 22. [[CrossRef](#)]
96. Samandari, L.; Bahrami, A.; Shamsipur, M.; Farzin, L.; Hashemi, B. Electrochemical preconcentration of ultra-trace Cd<sup>2+</sup> from environmental and biological samples prior to its determination using carbon paste electrode impregnated with ion imprinted polymer nanoparticles. *Int. J. Environ. Anal. Chem.* **2019**, *99*, 172–186. [[CrossRef](#)]
97. Hu, S.; Gao, G.; Liu, Y.; Hu, J.; Song, Y.; Zou, X. An Electrochemical Sensor Based on Ion Imprinted PPy/RGO Composite for Cd(II) Determination in Water. *Int. J. Electrochem. Sci.* **2019**, *14*, 11714–11730. [[CrossRef](#)]
98. Wang, J.; Hu, J.; Hu, S.; Gao, G.; Song, Y. A Novel Electrochemical Sensor Based on Electropolymerized Ion Imprinted PoPD/ERGO Composite for Trace Cd(II) Determination in Water. *Sensors* **2020**, *20*, 1004. [[CrossRef](#)]
99. Crapnell, R.D.; Banks, C.E. Electroanalytical overview: Utilising micro- and nano-dimensional sized materials in electrochemical-based biosensing platforms. *Mikrochim. Acta* **2021**, *188*, 268. [[CrossRef](#)] [[PubMed](#)]
100. Roy, E.; Patra, S.; Madhuri, R.; Sharma, P.K. Simultaneous determination of heavy metals in biological samples by a multiple-template imprinting technique: An electrochemical study. *RSC Adv.* **2014**, *4*, 56690–56700. [[CrossRef](#)]
101. Hart, J.P.; Wring, S.A. Recent developments in the design and application of screen-printed electrochemical sensors for biomedical, environmental and industrial analyses. *TrAC Trends Anal. Chem.* **1997**, *16*, 89–103. [[CrossRef](#)]
102. Metters, J.P.; Kadara, R.O.; Banks, C.E. New directions in screen printed electroanalytical sensors: An overview of recent developments. *Analyst* **2011**, *136*, 1067–1076. [[CrossRef](#)] [[PubMed](#)]
103. Crapnell, R.D.; Ferrari, A.G.-M.; Dempsey, N.C.; Banks, C.E. Electroanalytical overview: Screen-printed electrochemical sensing platforms for the detection of vital cardiac, cancer and inflammatory biomarkers. *Sens. Diagn.* **2022**, *1*, 405–428. [[CrossRef](#)]
104. Whittingham, M.J.; Hurst, N.J.; Crapnell, R.D.; Ferrari, A.G.-M.; Blanco, E.; Davies, T.J.; Banks, C.E. Electrochemical Improvements Can Be Realized via Shortening the Length of Screen-Printed Electrochemical Platforms. *Anal. Chem.* **2021**, *93*, 16481–16488. [[CrossRef](#)]
105. Kadara, R.O.; Jenkinson, N.; Banks, C.E. Characterisation of commercially available electrochemical sensing platforms. *Sens. Actuators B Chem.* **2009**, *138*, 556–562. [[CrossRef](#)]
106. Hayat, A.; Marty, J.L. Disposable Screen Printed Electrochemical Sensors: Tools for Environmental Monitoring. *Sensors* **2014**, *14*, 10432–10453. [[CrossRef](#)] [[PubMed](#)]
107. Li, M.; Li, Y.-T.; Li, D.-W.; Long, Y.-T. Recent developments and applications of screen-printed electrodes in environmental assays—A review. *Anal. Chim. Acta* **2012**, *734*, 31–44. [[CrossRef](#)] [[PubMed](#)]
108. Barton, J.; García, M.B.G.; Santos, D.H.; Fanjul-Bolado, P.; Ribotti, A.; McCaul, M.; Diamond, D.; Magni, P. Screen-printed electrodes for environmental monitoring of heavy metal ions: A review. *Mikrochim. Acta* **2016**, *183*, 503–517. [[CrossRef](#)]
109. Jamieson, O.; Soares, T.C.C.; de Faria, B.A.; Hudson, A.; Mecozzi, F.; Rowley-Neale, S.J.; Banks, C.E.; Gruber, J.; Novakovic, K.; Peeters, M.; et al. Screen Printed Electrode Based Detection Systems for the Antibiotic Amoxicillin in Aqueous Samples Utilising Molecularly Imprinted Polymers as Synthetic Receptors. *Chemosensors* **2019**, *8*, 5. [[CrossRef](#)]
110. Betlem, K.; Mahmood, I.; Seixas, R.; Sadiki, I.; Raimbault, R.; Foster, C.; Crapnell, R.; Tedesco, S.; Banks, C.; Gruber, J.; et al. Evaluating the temperature dependence of heat-transfer based detection: A case study with caffeine and Molecularly Imprinted Polymers as synthetic receptors. *Chem. Eng. J.* **2019**, *359*, 505–517. [[CrossRef](#)]
111. Silva, B.V.; Rodríguez, B.A.; Sales, G.F.; Sotomayor, M.; Dutra, R.F. An ultrasensitive human cardiac troponin T graphene screen-printed electrode based on electropolymerized-molecularly imprinted conducting polymer. *Biosens. Bioelectron.* **2016**, *77*, 978–985. [[CrossRef](#)] [[PubMed](#)]
112. Jamieson, O.; Betlem, K.; Mansouri, N.; Crapnell, R.; Vieira, F.; Hudson, A.; Banks, C.; Liauw, C.; Gruber, J.; Zubko, M.; et al. Electropolymerised molecularly imprinted polymers for the heat-transfer based detection of microorganisms: A proof-of-concept study using yeast. *Therm. Sci. Eng. Prog.* **2021**, *24*, 100956. [[CrossRef](#)]
113. Blanco-López, M.; Lobo-Castañón, M.; Miranda-Ordieres, A.; Tuñón-Blanco, P. Electrochemical sensors based on molecularly imprinted polymers. *TrAC Trends Anal. Chem.* **2004**, *23*, 36–48. [[CrossRef](#)]
114. McClements, J.; Tchekwagep, P.M.S.; Strapazon, A.L.V.; Canfarotta, F.; Thomson, A.; Czulak, J.; Johnson, R.E.; Novakovic, K.; Losada-Pérez, P.; Zaman, A.; et al. Immobilization of Molecularly Imprinted Polymer Nanoparticles onto Surfaces Using Different Strategies: Evaluating the Influence of the Functionalized Interface on the Performance of a Thermal Assay for the Detection of the Cardiac Biomarker Troponin I. *ACS Appl. Mater. Interfaces* **2021**, *13*, 27868–27879. [[CrossRef](#)] [[PubMed](#)]
115. McClements, J.; Bar, L.; Singla, P.; Canfarotta, F.; Thomson, A.; Czulak, J.; Johnson, R.E.; Crapnell, R.D.; Banks, C.E.; Payne, B.; et al. Molecularly Imprinted Polymer Nanoparticles Enable Rapid, Reliable, and Robust Point-of-Care Thermal Detection of SARS-CoV-2. *ACS Sens.* **2022**, *7*, 1122–1131. [[CrossRef](#)] [[PubMed](#)]
116. Peeters, M.M.; Van Grinsven, B.; Foster, C.W.; Cleij, T.J.; Banks, C.E. Introducing Thermal Wave Transport Analysis (TWTA): A Thermal Technique for Dopamine Detection by Screen-Printed Electrodes Functionalized with Molecularly Imprinted Polymer (MIP) Particles. *Molecules* **2016**, *21*, 552. [[CrossRef](#)]
117. Crapnell, R.D.; Hudson, A.; Foster, C.W.; Eersels, K.; van Grinsven, B.; Cleij, T.J.; Banks, C.E.; Peeters, M. Recent Advances in Electrosynthesized Molecularly Imprinted Polymer Sensing Platforms for Bioanalyte Detection. *Sensors* **2019**, *19*, 1204. [[CrossRef](#)] [[PubMed](#)]



118. Piletsky, S.A.; Piletskaya, E.V.; El'Skaya, A.; Levi, R.; Yano, K.; Karube, I. Optical Detection System for Triazine Based on Molecularly-Imprinted Polymers. *Anal. Lett.* **1997**, *30*, 445–455. [[CrossRef](#)]
119. Vlatakis, G.; Andersson, L.I.; Muller, R.S.; Mosbach, K. Drug assay using antibody mimics made by molecular imprinting. *Nature* **1993**, *361*, 645–647. [[CrossRef](#)] [[PubMed](#)]
120. Shariati, R.; Rezaei, B.; Jamei, H.R.; Ensafi, A.A. Application of coated green source carbon dots with silica molecularly imprinted polymers as a fluorescence probe for selective and sensitive determination of phenobarbital. *Talanta* **2019**, *194*, 143–149. [[CrossRef](#)]
121. Chmanguui, A.; Driss, M.R.; Touil, S.; Bermejo-Barrera, P.; Bouabdallah, S.; Moreda-Piñeiro, A. Aflatoxins screening in non-dairy beverages by Mn-doped ZnS quantum dots—Molecularly imprinted polymer fluorescent probe. *Talanta* **2019**, *199*, 65–71. [[CrossRef](#)]
122. Huang, K.; Chen, Y.; Zhou, F.; Zhao, X.; Liu, J.; Mei, S.; Zhou, Y.; Jing, T. Integrated ion imprinted polymers-paper composites for selective and sensitive detection of Cd(II) ions. *J. Hazard. Mater.* **2017**, *333*, 137–143. [[CrossRef](#)]
123. Lowdon, J.W.; Eersels, K.; Rogosic, R.; Heidt, B.; Diliën, H.; Redeker, E.S.; Peeters, M.; van Grinsven, B.; Cleij, T.J. Substrate displacement colorimetry for the detection of diarylethylamines. *Sens. Actuators B Chem.* **2018**, *282*, 137–144. [[CrossRef](#)]
124. Wu, M.; Deng, H.; Fan, Y.; Hu, Y.; Guo, Y.; Xie, L. Rapid Colorimetric Detection of Cartap Residues by AgNP Sensor with Magnetic Molecularly Imprinted Microspheres as Recognition Elements. *Molecules* **2018**, *23*, 1443. [[CrossRef](#)] [[PubMed](#)]
125. Zhao, B.; Feng, S.; Hu, Y.; Wang, S.; Lu, X. Rapid determination of atrazine in apple juice using molecularly imprinted polymers coupled with gold nanoparticles-colorimetric/SERS dual chemosensor. *Food Chem.* **2019**, *276*, 366–375. [[CrossRef](#)]
126. Kong, Q.; Wang, Y.; Zhang, L.; Ge, S.; Yu, J. A novel microfluidic paper-based colorimetric sensor based on molecularly imprinted polymer membranes for highly selective and sensitive detection of bisphenol A. *Sens. Actuators B Chem.* **2017**, *243*, 130–136. [[CrossRef](#)]
127. Li, C.; Ngai, M.H.; Reddy, K.K.; Leong, S.C.Y.; Tong, Y.W.; Chai, C.L.L. A fluorescence-displacement assay using molecularly imprinted polymers for the visual, rapid, and sensitive detection of the algal metabolites, geosmin and 2-methylisoborneol. *Anal. Chim. Acta* **2019**, *1066*, 121–130. [[CrossRef](#)] [[PubMed](#)]
128. Wagner, S.; Bell, J.; Biyikal, M.; Gawlitza, K.; Rurack, K. Integrating fluorescent molecularly imprinted polymer (MIP) sensor particles with a modular microfluidic platform for nanomolar small-molecule detection directly in aqueous samples. *Biosens. Bioelectron.* **2018**, *99*, 244–250. [[CrossRef](#)] [[PubMed](#)]
129. Wei, J.; Yuan, X.; Zhang, Y.; Liu, H.; Sun, B. Ionic liquid-sensitized molecularly imprinted polymers based on heteroatom co-doped quantum dots functionalized graphene for sensitive detection of  $\lambda$ -cyhalothrin. *Anal. Chim. Acta* **2020**, *1136*, 9–18. [[CrossRef](#)] [[PubMed](#)]
130. Hao, G.; Zhang, Z.; Ma, X.; Zhang, R.; Qin, X.; Sun, H.; Yang, X.; Rong, J. A versatile microfluidic paper chip platform based on MIPs for rapid ratiometric sensing of dual fluorescence signals. *Microchem. J.* **2020**, *157*, 105050. [[CrossRef](#)]
131. He, Y.; Hong, S.; Wang, M.; Wang, J.; El-Aty, A.M.A.; Hacimuftuoglu, A.; Khan, M.; She, Y. Development of fluorescent lateral flow test strips based on an electrospun molecularly imprinted membrane for detection of triazophos residues in tap water. *New J. Chem.* **2020**, *44*, 6026–6036. [[CrossRef](#)]
132. McNiven, S.; Kato, M.; Levi, R.; Yano, K.; Karube, I. Chloramphenicol sensor based on an in situ imprinted polymer. *Anal. Chim. Acta* **1998**, *365*, 69–74. [[CrossRef](#)]
133. Nicholls, C.; Karim, K.; Piletsky, S.; Saini, S.; Setford, S. Displacement imprinted polymer receptor analysis (DIPRA) for chlorophenolic contaminants in drinking water and packaging materials. *Biosens. Bioelectron.* **2006**, *21*, 1171–1177. [[CrossRef](#)]
134. Piletsky, S.A.; Terpetschnig, E.; Andersson, H.S.; Nicholls, I.A.; Wolfbeis, O.S. Application of non-specific fluorescent dyes for monitoring enantio-selective ligand binding to molecularly imprinted polymers. *Anal. Bioanal. Chem.* **1999**, *364*, 512–516. [[CrossRef](#)]
135. Greene, N.T.; Shimizu, K.D. Colorimetric Molecularly Imprinted Polymer Sensor Array using Dye Displacement. *J. Am. Chem. Soc.* **2005**, *127*, 5695–5700. [[CrossRef](#)]
136. Lowdon, J.; Diliën, H.; van Grinsven, B.; Eersels, K.; Cleij, T. Colorimetric Sensing of Amoxicillin Facilitated by Molecularly Imprinted Polymers. *Polymers* **2021**, *13*, 2221. [[CrossRef](#)]
137. Silverio, O.V.; So, R.C.; Elnar, K.J.S.; Malapit, C.A.; Nepomuceno, M.C.M. Development of dieldrin, endosulfan, and hexachlorobenzene-imprinted polymers for dye-displacement array sensing. *J. Appl. Polym. Sci.* **2017**, *134*. [[CrossRef](#)]
138. Haupt, K.; Mayes, A.A.G.; Mosbach, K. Herbicide Assay Using an Imprinted Polymer-Based System Analogous to Competitive Fluoroimmunoassays. *Anal. Chem.* **1998**, *70*, 3936–3939. [[CrossRef](#)]
139. Wan, W.; Descalzo, A.B.; Shinde, S.; Weißhoff, H.; Orellana, G.; Sellergren, B.; Rurack, K. Ratiometric Fluorescence Detection of Phosphorylated Amino Acids Through Excited-State Proton Transfer by Using Molecularly Imprinted Polymer (MIP) Recognition Nanolayers. *Chem. A Eur. J.* **2017**, *23*, 15974–15983. [[CrossRef](#)] [[PubMed](#)]
140. Wan, W.; Wagner, S.; Rurack, K. Fluorescent Monomers: “Bricks” That Make a Molecularly Imprinted Polymer “Bright”. *Anal. Bioanal. Chem.* **2016**, *408*, 1753–1771. [[CrossRef](#)]
141. Li, Q.; Shinde, S.; Grasso, G.; Caroli, A.; Hany, R.A.; Lanzillotta, M.; Pan, G.; Wan, W.; Rurack, K.; Sellergren, B. Selective detection of phospholipids using molecularly imprinted fluorescent sensory core-shell particles. *Sci. Rep.* **2020**, *10*, 9924. [[CrossRef](#)]
142. Turkewitsch, P.; Wandelt, B.; Darling, G.D.; Powell, W.S. Fluorescent Functional Recognition Sites through Molecular Imprinting. A Polymer-Based Fluorescent Chemosensor for Aqueous cAMP. *Anal. Chem.* **1998**, *70*, 2025–2030. [[CrossRef](#)]

143. Zhao, Y.; Ma, Y.; Li, H.; Wang, L. Composite QDs@MIP Nanospheres for Specific Recognition and Direct Fluorescent Quantification of Pesticides in Aqueous Media. *Anal. Chem.* **2012**, *84*, 386–395. [[CrossRef](#)]
144. Lin, C.I.; Joseph, A.K.; Chang, C.K.; Der Lee, Y. Molecularly imprinted polymeric film on semiconductor nanoparticles: Analyte detection by quantum dot photoluminescence. *J. Chromatogr. A* **2004**, *1027*, 259–262. [[CrossRef](#)]
145. Ren, X.; Liu, H.; Chen, L. Fluorescent detection of chlorpyrifos using Mn(II)-doped ZnS quantum dots coated with a molecularly imprinted polymer. *Mikrochim. Acta* **2015**, *182*, 193–200. [[CrossRef](#)]
146. Gerdan, Z.; Saylan, Y.; Uğur, M.; Denizli, A. Ion-Imprinted Polymer-on-a-Sensor for Copper Detection. *Biosensors* **2022**, *12*, 91. [[CrossRef](#)] [[PubMed](#)]
147. Wang, X.; Chu, Z.; Huang, Y.; Chen, G.; Zhao, X.; Zhu, Z.; Chen, C.; Lin, D. Copper Ion Imprinted Hydrogel Photonic Crystal Sensor Film. *ACS Appl. Polym. Mater.* **2022**, *4*, 4568–4575. [[CrossRef](#)]
148. Khoddami, N.; Shemirani, F. A new magnetic ion-imprinted polymer as a highly selective sorbent for determination of cobalt in biological and environmental samples. *Talanta* **2016**, *146*, 244–252. [[CrossRef](#)] [[PubMed](#)]
149. López, F.d.L.M.; Khan, S.; Picasso, G.; Sotomayor, M.D.P.T. A novel highly sensitive imprinted polymer-based optical sensor for the detection of Pb(II) in water samples. *Environ. Nanotechnol. Monit. Manag.* **2021**, *16*, 100497. [[CrossRef](#)]
150. Carboni, D.; Jiang, Y.; Malfatti, L.; Innocenzi, P. Selective detection of organophosphate through molecularly imprinted GERS-active hybrid organic-inorganic materials. *J. Raman Spectrosc.* **2018**, *49*, 189–197. [[CrossRef](#)]
151. Sullivan, M.V.; Allabush, F.; Bunka, D.; Tolley, A.; Mendes, P.M.; Tucker, J.H.R.; Turner, N.W. Hybrid aptamer-molecularly imprinted polymer (AptaMIP) nanoparticles selective for the antibiotic moxifloxacin. *Polym. Chem.* **2021**, *12*, 4394–4405. [[CrossRef](#)]
152. Ali, G.K.; Omer, K.M. Molecular imprinted polymer combined with aptamer (MIP-aptamer) as a hybrid dual recognition element for bio(chemical) sensing applications. Review. *Talanta* **2022**, *236*, 122878. [[CrossRef](#)]